NATIONAL TECHNICAL UNIVERSITY OF ATHENS

School of chemical engineering

Department of Process Analysis and Plant Designs

Thermodynamics and Transport Phenomena laboratory

Diploma Thesis

by

Cristina Carollo

Simulation of a natural gas TEG dehydration plant

Supervisors:

Epaminondas Voutsas, Associate Professor

Giuseppe Caputo, Associate Professor

Athens, June 2018

Acknowledgement

I would like to thank professor Voutsas for accepting me at NTUA and, in particular, at the Laboratory of Thermodynamics and Transport Phenomena, giving me the possibility to increase my knowledge on a field of my interest, which is natural gas.

I would like to thank professor Caputo for giving me the opportunity of doing my diploma thesis at NTUA with his collaboration.

I would first like to thank my supervisor Eirini Petropoulou for her infinite availability, for her attention in explaining what was necessary in a clear manner and for the interest placed in getting me to better conduct the present work.

I would like to thank the persons who work at the Erasmus+ offices of UNIPA and NTUA to have accepted me to participate to this program, allowing me to make a unique experience of its kind.

I would like to thank my friend Verdiana for having chosen to share this experience with me, allowing us to support each other when necessary and for not making me ever feel alone.

Finally, last but not least, I would like to thank my family and, in particular, my father, to have always believed in me and for always supporting me in the difficult moments of this university career and of my life, and having rejoiced with me when I reached goals, even if they were small.

LIST OF FIGURES

LIST OF TABLES

SUMMARY

Abstract

Natural gas is saturated with water at reservoir conditions. For this reason it is necessary to remove it to avoid operational problems, such as corrosion, hydrate formation or slug flow, during the transportation or processing of natural gas. This is usually obtained by dehydration, which is a process thanks to which water is removed from the gas to prevent its condensation under high pressure or low temperature conditions. Typically, in offshore units, dehydration by some glycol desiccant, usually triethylene glycol (TEG), occurs.

Although it is a generally used procedure in industrial practice, several parameters affect its efficiency, such as the glycol circulation rate, the operating conditions of the columns, the way by which the purity of the glycol is enhanced during regeneration etc. In particular, since it is not possible to work close to TEG boiling point, the lean TEG purity required by the absorption process is obtained in the regeneration section with enhanced methods, as the addition of stripping gas or setting vacuum conditions in the distillation column. For this reason, in this work, a sensitivity analysis of several operating variables of the process has been conducted. Namely, the effect of the temperature and pressure of the glycol contactor and regenerator, the temperature obtained after the heat exchangers and the stripping gas rate. This has been achieved by simulating a typical dehydration unit, based on conditions taken from the literature, in the Aspen HYSYS vs 8.8. environment. For the simulation two different thermodynamic models have been considered. That is the proposed by HYSYS for the use in dehydration TST-NRTL model and the UMR-PRU model which has been developed in the thermodynamics and transport phenomena laboratory and is known to yield satisfactory results for natural gas mixtures and it is implemented into HYSYS through the CAPE-OPEN 1.1 protocol.

From the sensitivity analysis, it has been established that an increase of the flash drum temperature and of the temperature of the stream which enters at the regenerator leads to a lower water content, with decrease of the required duties at the same time. For that reason, an optimization of the process in terms of required duties has been

conducted. The optimization occurred on the basis of a 30 ppm water content in the dry gas, as the required specification, which occurred using the stripping gas rate as independent variable. It is resulted that by increasing the temperature of the stream entering the regenerator to 137^{o}C and the flash drum temperature to 100^{o}C for the TST-NRTL or 90^{o}C for the UMR-PRU, there is an 9% decrease to the required reboiler duty for the first and a 8.2% decrease for the latter. This is also reflected to a 21% decrease in the stripping gas rate for the first and a 26% for the second. The cooler duty decreases as well at the optimized conditions, with a difference of 17% for TST-NRTL model and 14% with UMR-PRU. Instead, the duties of the two pumps are almost the same for both operating conditions.

Following the results of the sensitivity analysis, a preliminary economic evaluation of the unit is conducted in terms of installed and operating cost. The economic evaluation occurs for both the initial considered case and the optimized one, for each of the examined thermodynamic models. It is concluded that there is an about 5% difference between the obtained by HYSYS capital cost and the cost calculated through generalized correlations for each part of the equipment, while no significant difference is observed between base and optimized conditions. All obtained values are considered inside the uncertainty of the calculations and in good accordance with the available literature data, since the deviation in the case of the optimized simulation with UMR-PRU model is about 15 %, from the latter. Considering the operational costs, instead, a 8% decrease is obtained for the optimized conditions for the TST-NRTL model and 7% for the UMR-PRU, which corresponds to a saving of about 15700$/year.

Finally, the simulation of the dehydration of a real gas mixture occurred. It is concluded that both models are able to meet the required specification of 30 ppm of water content in the dry gas, yielding similar results with those observed in the synthetic gas case. The models differ in the calculated stripping gas rate. Actually, TST-NRTL results in higher stripping gas rate compared to UMR-PRU. The models differ, also, in the heavier components distribution in the glycol-rich streams, with UMR-PRU to

result generally in higher hydrocarbon loss. The same is valid for the calculated TEG loss.

From all the examined cases, it has been shown that the difference between the models is more profound in the calculated duties, where UMR-PRU systematically yields lower duty compared to TST-NRTL. Due to the better prediction of the aqueous TEG mixture heat capacity with the UMR-PRU model, its predictions in terms of duties are expected to be closer to the actual process data. Furthermore, UMR-PRU results in higher hydrocarbon loss in glycol-rich streams and higher TEG loss in the vapor stream which are closer to the corresponding phase equilibrium data.

Overall, it is concluded that the UMR-PRU model yields better results than the proposed by HYSYS TST-NRTL model in the simulation of a TEG dehydration unit.

Περίληψη

Το φυσικό αέριο περιέχει εκ φύσεως υδρατμούς σε συνθήκες ταμιευτήρα. Η απομάκρυνση του νερού από το αέριο είναι απαραίτητη ώστε να αποφευχθούν λειτουργικά προβλήματα κατά τις διεργασίες μεταφοράς και επεξεργασίας του αερίου. Η ύπαρξη του νερού, για παράδειγμα σε συνθήκες χαμηλής θερμοκρασίας και υψηλής πίεσης, όπως αυτές που επικρατούν στους υποθαλάσσιους αγωγούς μεταφοράς, μπορεί να οδηγήσει σε σχηματισμό υδριτών, ενώ παρουσία όξινων αερίων, μπορεί να οδηγήσει σε διαβρωτικές συνθήκες. Για την αποφυγή των παραπάνω, στη βιομηχανία του φυσικού αερίου είναι σύνηθες να προηγείται μία διεργασία αφυδάτωσης (dehydration). Στις υπεράκτιες πλατφόρμες παραγωγής αερίου, αυτό επιτυγχάνεται μέσω φυσικής απορρόφησης με χρήση ενός διαλύματος γλυκόλης, συνήθως τριαιθυλενογλυκόλης (TEG).

Αν και η διεργασία της αφυδάτωσης χρησιμοποιείται κατά κόρον στη βιομηχανία, αρκετές παράμετροι επηρεάζουν την ομαλή λειτουργία και την αποδοτικότητά της, όπως είναι ο ρυθμός κυκλοφορίας του διαλύματος γλυκόλης, οι λειτουργικές συνθήκες (πίεση, θερμοκρασία) των πύργων απορρόφησης και αναγέννησης, αντίστοιχα, οι θερμοκρασίες εισόδου στο δοχείο εκτόνωσης ή στον πύργο αναγέννησης κ.α.. Στην παρούσα διπλωματική εργασία πραγματοποιήθηκε ανάλυση ευαισθησίας ορισμένων λειτουργικών μεταβλητών που επηρεάζουν τη διεργασία. Πιο συγκεκριμένα, μελετήθηκε η επίδραση της θερμοκρασίας και της πίεσης λειτουργίας των πύργων απορρόφησης και αναγέννησης της γλυκόλης, η θερμοκρασία λειτουργίας του δοχείου εκτόνωσης και η θερμοκρασία εισόδου του ρεύματος της γλυκόλης στον πύργο αναγέννησης, καθώς και η επίδραση της παροχής του αερίου απογύμνωσης (stripping gas). Για την επίτευξη της παραπάνω ανάλυσης, μία τυπική μονάδα αφυδάτωσης φυσικού αερίου, βασισμένη σε λειτουργικά δεδομένα που λήφθηκαν από τη βιβλιογραφία, προσομοιώθηκε στο περιβάλλον του Aspen HYSYS vs 8.8, βασισμένο σε μοντέλο ισορροπίας. Για την περιγραφή των θερμοδυναμικών ιδιοτήτων του συστήματος, μελετήθηκαν δύο διαφορετικά θερμοδυναμικά μοντέλα: το προτεινόμενο από το HYSYS για χρήση σε τέτοιες διεργασίες TST-NRTL και ένα μοντέλο που έχει

αναπτυχθεί στο εργαστήριο θερμοδυναμικής και φαινομένων μεταφοράς του ΕΜΠ και δίνει καλά αποτελέσματα σε μίγματα φυσικών αερίων, το UMR-PRU. Το τελευταίο, δεν είναι ενσωματωμένο σε εμπορικούς προσομοιωτές, οπότε εισάγεται σε αυτούς μέσω του πρωτοκόλλου CAPE OPEN 1.1.

Από τα αποτελέσματα των αναλύσεων ευαισθησίας προέκυψε ότι η αύξηση της θερμοκρασίας εισόδου στο δοχείο εκτόνωσης καθώς και η θερμοκρασία εισόδου του ρεύματος γλυκόλης στον αναγεννητή, μπορεί να βελτιώσει την απομάκρυνση του νερού από το αέριο με ταυτόχρονη μείωση του απαιτούμενου θερμικού φορτίου στον αναβραστήρα της στήλης αναγέννησης. Βάσει των παραπάνω, πραγματοποιήθηκε αριστοποίηση της διεργασίας με στόχο τη μείωση των απαιτούμενων φορτίων και ως εκ τούτου, εμμέσως του λειτουργικού κόστους της μονάδας. Για το σκοπό της αριστοποίησης θεωρήθηκε μία προδιαγραφή 30 ppm νερού στο ρεύμα του ξηρού αερίου, που επιτεύχθηκε με τη χρήση της ροής αερίου απογύμνωσης ως ανεξάρτητης μεταβλητής. Τα αποτελέσματα της βελτιστοποίησης έδειξαν ότι η αύξηση της θερμοκρασίας εισόδου στον αναγεννητή στους 137^{o}C και της θερμοκρασίας λειτουργίας του δοχείου εκτόνωσης στους 100^{o}C για το TST-NRTL και στους 90^{o}C για το UMR-PRU, οδηγεί σε 9% μείωση θερμικού φορτίου του αναβραστήρα της στήλης αναγέννησης για το πρώτο και 8.2% για το δεύτερο. Αυτή η μείωση, οδηγεί και σε αντίστοιχη μείωση του απαιτούμενου αερίου απογύμνωσης, που είναι 21% για το πρώτο και 26% στην περίπτωση του δεύτερου. Επιπλέον, παρατηρείται μείωση του απαιτούμενου φορτίου στον ψυκτήρα γλυκόλης κατά 17% για το TST-NRTL και 21% για το UMR-PRU, κατά τις αριστοποιημένες συνθήκες λειτουργίας.

Στη συνέχεια, πραγματοποιήθηκε προκαταρκτική οικονομική ανάλυση της διεργασίας, χρήσει και των δύο θερμοδυναμικών μοντέλων, σε συνθήκες βάσης και αριστοποίησης. Η ανάλυση βασίστηκε στα πάγια κόστη εγκατάστασης και στο λειτουργικό κόστος, όπως αυτό προκύπτει από τις απαιτούμενες παροχές σε θέρμανση, ψύξη και ηλεκτρισμό. Δύο μέθοδοι χρησιμοποιήθηκαν για την επίτευξη αυτού του σκοπού: η οικονομική ανάλυση από το περιβάλλον του HYSYS καθώς και αναλυτικός υπολογισμός του κόστους κάθε τμήματος εξοπλισμού βασισμένο σε συσχετίσεις της

βιβλιογραφίας. Τα αποτελέσματα της ανάλυσης ως προς το πάγιο κόστος εγκατάστασης έδειξαν ότι δεν υπάρχει σημαντική διαφοροποίηση μεταξύ των βασικών συνθηκών λειτουργίας και των βελτιστοποιημένων. Μεταξύ, όμως, των τιμών που υπολογίστηκαν από το λογισμικό HYSYS ICARUS και τις γενικευμένες συσχετίσεις προκύπτει μία διαφορά ίση με περίπου 5% σε όλες τις μελετούμενες περιπτώσεις. Οι διαφορές αυτές θεωρούνται λογικές δεδομένου του προκαταρκτικού σχεδιασμού και των απλοποιητικών παραδοχών που πραγματοποιήθηκαν. Επιπλέον, οι υπολογισμένες τιμές είναι συγκρίσιμες με τιμές που δίνονται στη βιβλιογραφία για το κόστος μίας τέτοιας μονάδας. Πιο συγκεκριμένα, τα υπολογισμένα κόστη για τις αριστοποιημένες συνθήκες λειτουργίας με το UMR-PRU μοντέλο αποκλίνουν κατά περίπου 15% από τις βιβλιογραφικές τιμές. Όσον αφορά στον υπολογισμό του λειτουργικού κόστους της μονάδας, παρατηρείται μία σημαντική μείωση του κόστους στην περίπτωση των αριστοποιημένων συνθηκών και με τα δύο μελετούμενα μοντέλα. Ειδικότερα, στην περίπτωση του TST-NRTL το λειτουργικό κόστος μειώνεται κατά 8%, ενώ σε αυτή του UMR-PRU κατά 7%. Αυτή η μείωση αντιστοιχεί σε περιθώριο κέρδους σε ετήσια βάση κατά περίπου 15700$.

Τέλος, πραγματοποιήθηκε προσομοίωση μίας μονάδας αφυδάτωσης που τροφοδοτείται με πραγματικό αέριο και με τα δύο εξεταζόμενα θερμοδυναμικά μοντέλα. Η ανάλυση έγινε και σε αυτή την περίπτωση στη βάση της προδιαγραφής των 30 ppm νερού στο παραγόμενο ξηρό αέριο, που και τα δύο μοντέλα προσομοίωσαν επιτυχώς. Τα αποτελέσματα που παρατηρήθηκαν είναι παρόμοια με αυτά του συνθετικού αερίου. Ειδικότερα, τα μοντέλα απαιτούν τον ίδιο ρυθμό ανακυκλοφορίας γλυκόλης και την ίδια καθαρότητα γλυκόλης για την επίτευξη της προδιαγραφής. Ωστόσο, και σε αυτή την περίπτωση το UMR-PRU απαιτεί μικρότερη ροή αερίου απογύμνωσης, συγκρινόμενο με το TST-NRTL. Όπως και στην περίπτωση του συνθετικού αερίου, το UMR-PRU μοντέλο οδηγεί σε κατά περίπου 19% μικρότερο φορτίο. Επιπλέον, τα μοντέλα διαφέρουν ως προς την κατανομή των βαρύτερων συστατικών στα πολικά ρεύματα, με το UMR-PRU να οδηγεί σε υψηλότερες διαλυτότητες και άρα και μεγαλύτερη απώλεια υδρογονανθράκων. Το ίδιο ισχύει και για τις απώλειες της TEG στο ρεύμα του αερίου.

Τέλος, σε όλες τις προηγούμενες αναλύσεις αποδείχθηκε ότι η σημαντικότερη διαφοροποίηση στην πρόβλεψη των μοντέλων έγκειται στον υπολογισμό των απαιτούμενων θερμικών φορτίων, όπου το UMR-PRU συστηματικά προβλέπει μικρότερες τιμές. Αυτό αποδίδεται στην πρόβλεψη της ειδικής θερμοχωρητικότητας που είναι συστηματικά μικρότερη στην περίπτωση του UMR-PRU σε σχέση με αυτή που υπολογίζεται μέσω του TST-NRTL. Επειδή η πρόβλεψη του UMR-PRU είναι καλύτερη στην περίπτωση της ειδικής θερμοχωρητικότητας του υδατικού μίγματος TEG, θεωρείται ότι τα αποτελέσματά του ως προς την πρόβλεψη των απαιτούμενων φορτίων θα είναι πιο κοντά στις πραγματικές τιμές. Επιπλέον, οι προβλέψεις των μοντέλων διαφοροποιούνται ως προς τις απώλειες υδρογονανθράκων στο ρεύμα γλυκόλης και TEG στα αέρια ρεύματα, όπου το UMR-PRU συστηματικά καταλήγει σε μεγαλύτερες τιμές. Λόγω της καλύτερης πρόβλεψης της ισορροπίας φάσεων των αντίστοιχων δυαδικών μιγμάτων, τα αποτελέσματα του UMR-PRU θεωρούνται ότι θα είναι πιο κοντά στις πραγματικές τιμές.

Συνοψίζοντας, στην παρούσα εργασία αποδείχθηκε ότι το μοντέλο UMR-PRU μπορεί να προσομοιώσει επιτυχώς μία διεργασία αφυδάτωσης φυσικού αερίου, οδηγώντας σε παρόμοια και σε ορισμένες περιπτώσεις καλύτερα αποτελέσματα συγκρινόμενο με αυτά που υπολογίζονται μέσω του μοντέλου TST-NRTL που προτείνεται από το HYSYS για την προσομοίωση τέτοιων διεργασιών.

1. Scope

Natural gas is a combustible mixture of hydrocarbon gases, mostly methane, ethane, propane, butane and pentane [1], but it also is saturated with water at reservoir conditions. A necessary step to avoid operational problems during its transportation or processing is its dehydration. [2]

Although the dehydration procedure is generally used in industrial practice, several parameters affect its efficiency, such as the glycol circulation rate, the operating conditions of the columns, the way by which the purity of the glycol is enhanced during regeneration etc. To that purpose, in this work, a sensitivity analysis of several operating variables of the process has been conducted. The sensitivity analysis aims also at the establishing of optimised operational conditions in terms of reducing the required thermal duties. For this reason, a specification of 30 ppm water content in the dry gas has been set, while the independent variable is the stripping gas rate. Following the optimisation of the operating conditions, a preliminary economic evaluation of the unit in terms of installed and operating cost occurs. Finally, in contradiction to the synthetic gas used for the sensitivity analysis, a real gas is examined.

The simulations have been conducted through the Aspen HYSYS vs 8.8 software, with the use of two different thermodynamic models. The models considered are the built-in TST-NRTL model [3] [4] which is proposed by HYSYS to be used in simulating the dehydration process and the UMR-PRU model [5] [6] which has been shown to yield good results in natural gas mixtures. [7] The latter is implemented into HYSYS through the CAPE-OPEN 1.1 protocol.

1.1 References

[1] Jacob N.C.G., Optimization of triethylene glycol (TEG) dehydration in a natural gas processing plant, International Journal of Research in Engineering and Technology, 2014, 3, 346-350

[2] Gandhidasan P., Parametric analysis of natural gas dehydration by a triethylene glycol solution, Energy Sources, 2003, 25, 189-201.

[3] Twu C.H., Sim W.D., Tassone V., Liquid activity coefficient model for CEOS/AE mixing rules, Fluid Phase Equilibria 2001, 183–184, 65-74.

[4] Twu C.H., Sim W.D., Tassone V., A versatile liquid activity model for SRK, PR and a new cubic equation-of-state TST, Fluid Phase Equilibria 2002, 194–197, 385-399.

[5] Voutsas, E., Louli V., Boukouvalas C., Magoulas K.,Tassios D., Thermodynamic property calculations with the universal mixing rule for EoS/GE models: Results with the Peng–Robinson EoS and a UNIFAC model. Fluid Phase Equilibria 2006, 241, (1–2), 216-228

[6] Voutsas E., Magoulas K., Tassios D., Universal Mixing Rule for Cubic Equations of State Applicable to Symmetric and Asymmetric Systems: Results with the Peng−Robinson Equation of State. Industrial & engineering chemistry research 2004, 43, (19), 6238-6246

[7] Louli V., Pappa G., Boukouvalas C., Skouras S., Solbraa E., Christensen K. O., Voutsas E., Measurement and prediction of dew point curves of natural gas mixtures, Fluid Phase Equilibria 2012, 334, 1-9.

2. Theoretical background

2.1 Operational problems due to the presence of water in naturals gas

Natural gas (NG) is saturated with water at reservoir conditions. Since water vapor could condense under high pressure and low temperature, it is necessary to remove it to avoid some operating issues during natural gas transportation and processing. Such issues include:

- *Hydrate formation*: liquid water and light hydrocarbons may form hydrates, which lead to the partial or complete blocking of pipes and downstream equipment, fouling, plugging of heat exchangers and erosion of many processing equipment.
- *Corrosion*: in the presence of water, hydrogen sulfide and carbon dioxide form weak corrosive acids.
- *Slug flow*: liquid water may cause slugging which lead to the damage of downstream equipment. [1]

To avoid such operational points, water has to be removed from the gas to meet some established specifications. In terms of industrial practice this is usually established as water dew point temperature, which actually can be translated to ppm of water content. The specification to be met in this work is the water dew point temperature of -18 ^{o}C, which is the usual specification for transportation pipelines in Northern Europe and corresponds to a dry gas water content of about 30 ppm. [2] Offshore, this specification is typically obtained by absorption of water in some glycol desiccant. In most cases, triethylene glycol (TEG) is used, which yields the best combination in terms of cost and efficiency. [3]

2.2 Absorption of water from NG using TEG

A typical offshore processing plant for natural gas is shown in Figure 2.1 [2].

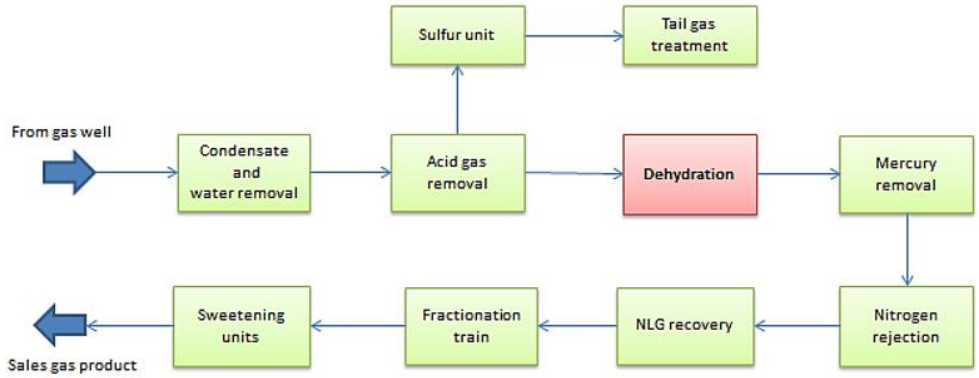

Figure 2. 1 Typical processing plant for natural gas [2]

Due to lack of space in offshore units, only the basic processing to meet the specifications of the transportation pipelines is used. As it is shown in Figure 2.1, this typically involves the removal of water, mercury and acid gases (H_2S, CO_2). The latter appears only where high concentrations of acid gases are involved, while in other cases the processing occurs onshore. In case that a sweetening unit exists, this should always be placed before dehydration, since it typically uses a mixture of water and amines.

The most commonly used method for natural gas dehydration offshore is an absorption process. The solvent should have the following properties:

- Strong affinity to water and low affinity for hydrocarbons
- Low volatility
- Low cost
- Low viscosity
- Low tendency to form foams or emulsions
- Low potential for corrosion
- Large difference in boiling point compared to water [2]

Four glycols are used for dehydration process:

- Monoethylene glycol (MEG)
- Diethylene glycol (DEG)
- Triethylene glycol (TEG)
- Tetraethylene glycol (TeEG) [4]

TEG is the most commonly used glycol for gas dehydration, because it gives the best combination of dew point depression, operating cost and reliability. In particular, this thesis focuses on natural gas dehydration with TEG as absorbent. TEG has a boiling point (287.8°C) at atmospheric pressure that is much higher than the one of water (100°C). This difference comes handy in order to ensure easy separation of the rich TEG stream, just by increasing the temperature in the regenerator. [4]

2.3 Thermodynamic models

For the simulation of the typical TEG dehydration unit in HYSYS, the equilibrium approach is followed. So, important role plays the selected thermodynamic model. In this work, two models are examined which belong to the so-called class of the EoS/G^E class, namely the Twu-Sim-Tassone Non Random Twu Liquid (TST-NRTL) [5] [6] which is proposed by HYSYS for use in the dehydration process and the Universal Mixing Rule Peng – Robinson UNIFAC [7] [8] (UMR-PRU) which has been shown to yield very satisfactory results in the prediction of natural gas mixtures[9]. The latter is implemented into HYSYS through the CAPE OPEN 1.1 protocol.

2.3.1 TST-NRTL model

The cubic EoS/A^E mixing rule combines the Twu –Sim-Tassone (TST) EoS [10] with the NRTL[11] model through zero-pressure mixing rules. The TST cubic equation of state is represented by the following expression [12]:

$$P = \frac{RT}{v-b} - \frac{a}{(v+3\cdot b)(v-0.5\cdot b)} \quad \text{Eq. (2.1)}$$

$$a = \mathrm{a_c}\ \mathrm{a(T)} \quad \text{Eq. (2.2)}$$

$$\mathrm{a_c} = 0.470507\frac{(RT_c)^2}{P_c} \quad \text{Eq. (2.3)}$$

$$\mathrm{a}(T) = T_r^{N(M-1)} e^{L(1-T_r^{NM})} \quad \text{Eq. (2.4)}$$

$$b = 0.0740740\frac{RT_c}{P_c} \quad \text{Eq. (2.5)}$$

where T_c and P_c are the compound critical temperature and pressure, and L, M and N are compound specific pure component parameters fitted to vapor pressure data.

The zero pressure mixing rules are expressed by **Error! Reference source not found.**eqs. 2.6 - 2.11. The TST zero-pressure mixing rules assume that the excess Helmholtz energy of the van der Waals fluid at zero pressure, $A^E_{0,vdw}$, can be approximated by the excess Helmholtz energy of the van der Waals fluid at infinite pressure, $A^E_{\infty,vdw}$, as in eq. 2.9.

$$a^* = b^*\left[\frac{a^*_{vdw}}{b^*_{vdw}} + \frac{1}{-0.518850}\left(\frac{A^E_0}{RT} - \frac{A^E_{0,vdw}}{RT}\right)\right] \quad \text{Eq. (2.6)}$$

$$a^* = \frac{Pa}{(RT)^2} \quad \text{Eq. (2.7)}$$

$$b^* = \frac{Pb}{RT} \quad \text{Eq. (2.8)}$$

$$\frac{A^E_{0,vdw}}{RT} = \frac{A^E_{\infty,vdw}}{RT} = -0.59413 \cdot \left[\frac{a^*_{vdw}}{b^*_{vdw}} + \sum_i x_i \frac{a^*_i}{b^*_i}\right] \quad \text{Eq. (2.9)}$$

$$b = b_{vdw} = \sum_i \sum_j x_i x_j \, b_{ij} \;\text{ with }\; b_{ij} = \frac{b_i + b_j}{2} \quad \text{Eq. (2.10)}$$

$$a_{vdw} = \sum_i \sum_j x_i x_j a_{ij} \;\; with \;\; a_{ij} = \sqrt{a_i a_j}(1 - k_{ij}) \quad \text{Eq. (2.11)}$$

Since A_0^E in eq. 2.6**Error! Reference source not found.** is at zero-pressure, its value is identical to the excess Gibbs free energy G^E at zero-pressure. Twu et al. [11] proposed a multicomponent equation for G^E that has the same structural form with the NRTL activity coefficient model, as shown in 2.12 - 2.14.

$$\frac{G^E}{RT} = \sum_i^n x_j \frac{\sum_j^n x_j \tau_{ji} G_{ji}}{\sum_k^n x_k G_{ki}} \quad \text{Eq. (2.12)}$$

$$\tau_{ji} = \frac{A_{ji}}{T} + B_{ji} \quad \text{Eq. (2.13)}$$

$$G_{ji} = \exp(-\alpha_{ji}\tau_{ji}) \quad \text{Eq. (2.14)}$$

where A_{ji}, B_{ji} and α_{ji} are the NRTL interaction parameters. The pure component and binary interaction parameters for the TEG/water binary mixture are taken from Twu et al. [11] while for the rest from the HYSYS vs 8.8 database.

2.3.2 UMR-PRU model

The UMR-PRU model, combines the Peng-Robinson Equation of State with the UNIFAC activity coefficient model, through the Universal Mixing Rules [7 - 8]. The

model has been shown to be applicable to all types of system asymmetries and to yield good results for natural gas mixtures [9 - 13].

The Peng-Robinson EoS in terms of pressure is given by the following expression:

$$P = \frac{RT}{(v-b)} - \frac{a}{v(v+b)+b(v-b)} \qquad \text{Eq. (2.15)}$$

$$a = \mathrm{a_c}\,\mathrm{a(T)} \qquad \text{Eq. (2.16)}$$

$$\mathrm{a_c} = 0.45724\frac{(\mathrm{RT_c})^2}{\mathrm{P_c}} \qquad \text{Eq. (2.17)}$$

$$\mathrm{a}(T) = [1 + m(1 - T_r^{0.5})]^2 \qquad \text{Eq. (2.18)}$$

$$m = 0.37464 + 1.54226\omega - 0.26992\omega^2 \qquad \text{Eq. (2.19)}$$

$$b = 0.07780\frac{RT_c}{P_c} \qquad \text{Eq. (2.20)}$$

where T_c and P_c are the compound critical temperature and pressure respectively and ω is the acentric factor.

For extension to mixtures the following Universal Mixing Rules (UMR) proposed by Voutsas et al are applied [8]:

$$\frac{a}{bRT} = \frac{1}{-0.53}\frac{G_{AC}^{E,SG} + G_{AC}^{E,res}}{RT} + \sum_{\mathrm{i}} x_i \frac{\mathrm{a_i}}{b_i RT} \qquad \text{Eq. (2.21)}$$

$$b = \sum_i \sum_j x_i x_j\, b_{ij} \text{ with } b_{ij} = \left(\frac{b_i^{1/2} + b_j^{1/2}}{2}\right)^2 \qquad \text{Eq. (2.22)}$$

2.4 Process Description

For simulation purposes Aspen HYSYS software has been used. The flowsheet of a typical dehydration unit, as simulated on HYSYS, is shown in Figure 2.2.

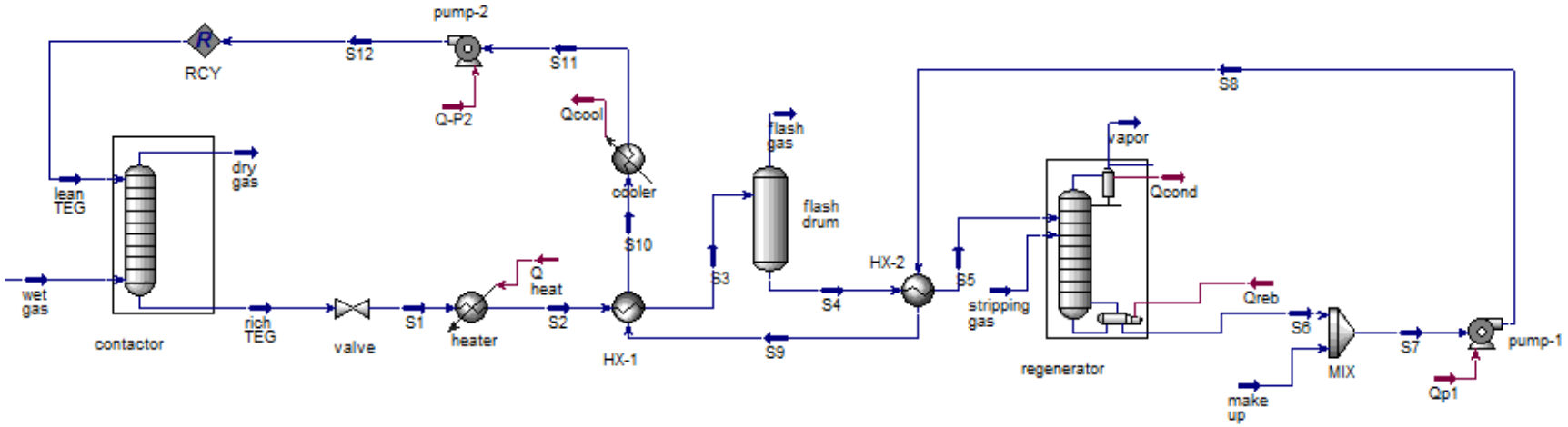

Figure 2. 2 Flowsheet of a dehydration unit as simulated on HYSYS.

The dehydration unit is composed of two parts: an *absorption* section, where dehydration takes place, and a *regeneration* section, where water is separated from TEG. In the absorption section the actual dehydration occurs. At the top exits the final product of the unit, which is actually the dry gas stream, and at the bottom the rich (in water) TEG stream, which is then routed for regeneration. The regeneration is actually a stripping process, where by attributing heat, water is separated from the rich TEG stream. The produced lean (in water) TEG stream, is then recycled as an input at the top of the absorber [2]. For the base condition case, from where the sensitivity analysis occurred, the input and operating conditions have been taken from the work of dos Santos et al.[14]. The detailed composition of the input wet gas stream is given in Table 2.1. The base conditions are described in the following, while any difference which may occur during the sensitivity analysis is discussed in section 3.

Table 2.1: Wet gas composition (molar)

	Wet gas	Stripping gas	Make-up
CO_2	1.39 E-02	1.82 E-01	-
Methane	8.99 E-01	7.27 E-01	-
Ethane	6.54 E-02	9.1 E-02	-
Propane	1.75 E-02	-	-
n-Butane	2.44 E-03	-	-
n-Pentane	7.24 E-04	-	-
n-Hexane	5.51 E-04	-	-
H_2O	3.94 E-04	-	5.00 E-03
TEG	-	-	9.95 E-01

2.4.1 Absorption section

An absorber unit (Contactor), which consists of three ideal trays, operates at high pressure and low temperature conditions, in this case about 52 bar and 27^{o}C [7], and it is essentially isothermal. Since the mass of the lean TEG which enters at the top of the contactor is small compared to that of the wet gas which enters at the bottom, with a flowrate equal to 1904 kmol/h, the absorber temperature is controlled by the wet gas one. From the top of the contactor exits the dry gas which is the final product of the unit and, from the bottom, exits the rich TEG stream which is then routed into the regeneration section.

2.4.2 Regeneration section

The rich TEG stream from the contactor is depressurized in a Joule-Thomson valve from 51.65 bar to 5.15 bar, since the regenerator works close to the atmospheric pressure. For simulation purposes, a heater is added next to the valve, and its duty is set equal to that of the condenser, to account for the passing of the rich TEG stream from the condenser of the Regenerator. The rich TEG is then preheated through the first glycol/glycol heat exchanger (HX-1) by the lean TEG stream and it is then routed to a flash drum to remove the diluted hydrocarbons, in order to pretreat it before the regeneration. The liquid outlet stream (S4) enters the second glycol/glycol heat exchanger (HX-2), with a specified temperature equal to 130^{o}C, before it enters the bottom of the Regenerator.

The latter is simulated by a distillation column subflowsheet which operates at close to atmospheric pressure (1.27 bar) and high temperature conditions, due to the high TEG boiling point (285°C). For the condenser the "full reflux" option has been chosen, so that all the condensed liquid is sent back to the top of the regenerator. The number of stages has been set to three without accounting for the reboiler and the condenser. The operating conditions of the regenerator have been defined by the glycol degradation temperature, so the specifications for the column are set to the reboiler and condenser temperature. For this reason, the condenser temperature is set to 100^{o}C,

which is close to the pure water boiling point, while for the reboiler one it is set to 204.6°C, which is the best compromise between increasing the lean TEG purity and avoiding the TEG degradation. [4] Since this temperature corresponds to a lean TEG purity of about 98.5% wt. [4], in the typical case, where a specific water content in the dry gas is required and corresponds to higher TEG purity (about 99.5% wt. [4]), this is obtained with the use of a stripping gas. Although several approaches can be used for the stripping gas, such as some of the produced dry natural gas, pure methane, pure CO_2 etc., in this work a stripping gas composition taken from the work of dos Santos et al.[14] is used, as it is presented in Table 2.1.

To account for the TEG losses encountered at the dry gas, the flash gas and the vapor, streams, a make-up stream of aqueous TEG is added with a wt. composition equal to 0.995 in TEG (Table 2.1). The conditions of the lean TEG stream are set to those required in the Contactor through the use of auxiliary units, which are actually, two glycol pumps (pump-1, pump-2) and a glycol cooler (cooler).

2.5 References

[1] Jacob N. C. G., Optimization of triethylene glycol (TEG) dehydration in a natural gas processing plant, International Journal of Research in Engineering and Technology, 2014, 3, 346-350

[2] Husby B. K., Simulation of TEG dehydration plants, master thesis at Norwegian University of Science and Technology Department of Energy and Process Engineering, 2014

[3] Gandhidasan, P., Parametric analysis of natural gas dehydration by a triethylene glycol solution. Energy Sources 25 (2003) 189-201.

[4] Campbell, J.M. and Maddox R.N., Gas conditioning and processing. Vol. 2. Campbell Petroleum Series. 1970.

[5] Twu C.H., Sim W.D., Tassone V., Liquid activity coefficient model for CEOS/AE mixing rules, Fluid Phase Equilibria 2001, 183–184, 65-74.

[6] Twu C.H., Sim W.D., Tassone V., A versatile liquid activity model for SRK, PR and a new cubic equation-of-state TST, Fluid Phase Equilibria 2002, 194–197, 385-399.

[7] Voutsas, E., Louli V., Boukouvalas C., Magoulas K.,Tassios D., Thermodynamic property calculations with the universal mixing rule for EoS/GE models: Results with the Peng–Robinson EoS and a UNIFAC model. Fluid Phase Equilibria 2006, 241, (1–2), 216-228

[8] Voutsas E., Magoulas K., Tassios D., Universal Mixing Rule for Cubic Equations of State Applicable to Symmetric and Asymmetric Systems: Results with the Peng−Robinson Equation of State. Industrial & engineering chemistry research 2004, 43, (19), 6238-6246

[9] Louli V., Pappa G., Boukouvalas C., Skouras S., Solbraa E., Christensen K. O., Voutsas E., Measurement and prediction of dew point curves of natural gas mixtures, Fluid Phase Equilibria 2012, 334, 1-9.

[10] Twu C.H., Coon J.E., Bluck D., Equations of state using an extended Twu-Coon mixing rule incorporating UNIFAC for high temperature and high pressure phase equilibrium predictions. Fluid Phase Equilibria 1997, 139, (1–2), 1-13.

[11] Twu C.H., Tassone V., Sim W.D., Watanasiri S., Advanced equation of state method for modeling TEG–water for glycol gas dehydration. Fluid Phase Equilibria 2005, 228–229, 213-221.

[12] Twu C. H., Bluck, D., Cunningham J. R., Coon J. E., A cubic equation of state with a new alpha function and a new mixing rule. Fluid Phase Equilibria 1991, 69, 33-50.

[13] Skylogianni, E., Novak, N., Louli, V., Pappa, G., Boukouvalas, C., Skouras, S., Solbraa, E., Voutsas, E., Measu rement and prediction of dew points of six natural gases. Fluid Phase Equilibria 2015.

[14] Dos Santos L.C., Abunahman S.S., Tavares F.W., Ruiz Ahón V.R., Kontogeorgis G.M., *Cubic Plus Association Equation of State for Flow Assurance Projects*, Industrial & Engineering Chemistry Research, 2015, 54, 6812-6824.

3. Sensitivity analysis

The scope of the sensitivity analysis is to evaluate the influence of the operating parameters such as temperature, pressure and stripping gas rate on the whole process. The abovementioned analysis aims to an optimization from an energetic point of view, the latter on the basis of the specification of dry gas water content at approximately 30 ppm molar.

A base case, as it is described in Section 2.4, has been considered, with the operating conditions presented on Table 3.1 [1].

Table 3 .1 Base operating conditions inserted as input for the simulation of the base case with TST-NRTL and UMR-PRU models[1]

Contactor temperature [ºC]	26.67
Contactor pressure [bar]	51.65
Wet gas molar flow [kmol/h]	1904
S1 pressure [bar]	5.15
Flash drum temperature [ºC]	75
Flash drum pressure [bar]	3.15
Input regenerator temperature [ºC]	130
S8 pressure [bar]	3.77
Stripping gas temperature [ºC]	80
Stripping gas pressure [bar]	2
Stripping gas molar flow [kmol/h]	7
S11 temperature [ºC]	55
S12 pressure [bar]	52
Make-up temperature [ºC]	15
Make-up pressure [bar]	2

The effect of the operational variables has been analyzed, by varying the specific parameter, while all the rest have been kept constant to the value of the base conditions. Exception is encountered in the case of the variation of the Regenerator pressure, where no stripping gas is considered. Although the scope of the sensitivity analysis is to study the effect of each operating parameter on the process, particular emphasis has been given in checking the conditions where the specification of the about 30 ppm water in the dry gas is satisfied.

3.1 Variation of the stripping gas molar flow

Stripping gas has been used in the regeneration section to increase the lean TEG purity, since it is not possible to work close to TEG boiling point due to its degradation temperature being lower to its boiling point. The effect of the variation of the stripping gas rate has been analyzed in this section.

Figure 3.1 shows the trend of the lean TEG purity after variations of the stripping gas molar flow. As it has been expected, there is an increase of the lean TEG purity with the increase of stripping gas rate with both the models. A slight difference in the lean TEG purity is observed between UMR-PRU and TST-NRTL, which is more apparent in the lower stripping gas rate. This is attributed to the different performance of the two models in the vapor – liquid equilibrium (VLE) of natural gas components with water and TEG.

Figure 3.2 shows the trend of the dry gas water content after variations of the stripping gas molar flow. As expected from the results in the purity of the lean TEG, the dry gas water content decreases with the increase of stripping gas, due to the higher absorbing capacity of the solvent. If the performance of the models in meeting the required specification of 30 ppm of water in the dry gas is examined, it is observed that UMR-PRU requires slightly lower rate compared to TST-NRTL.

.

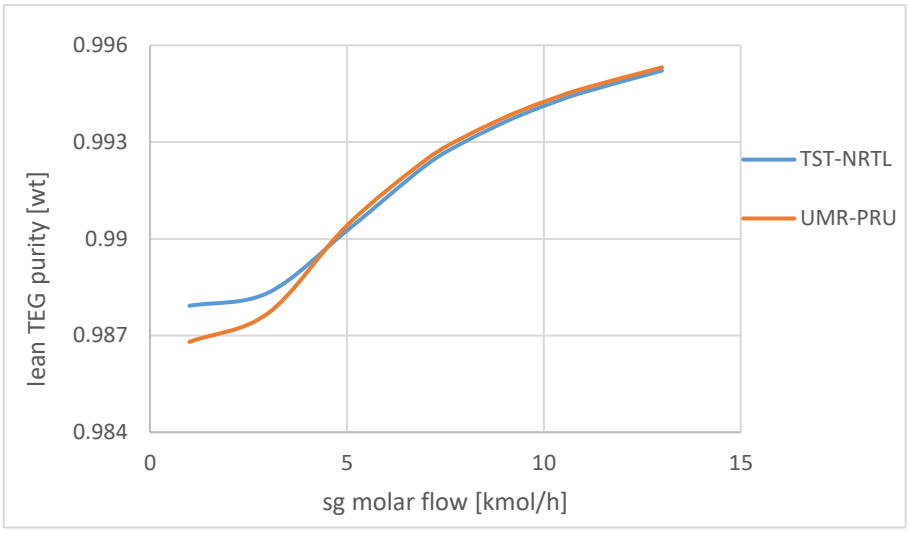

Figure 3.1 Effect of the stripping gas rate on the lean TEG purity with the TST-NRTL and the UMR-PRU models.

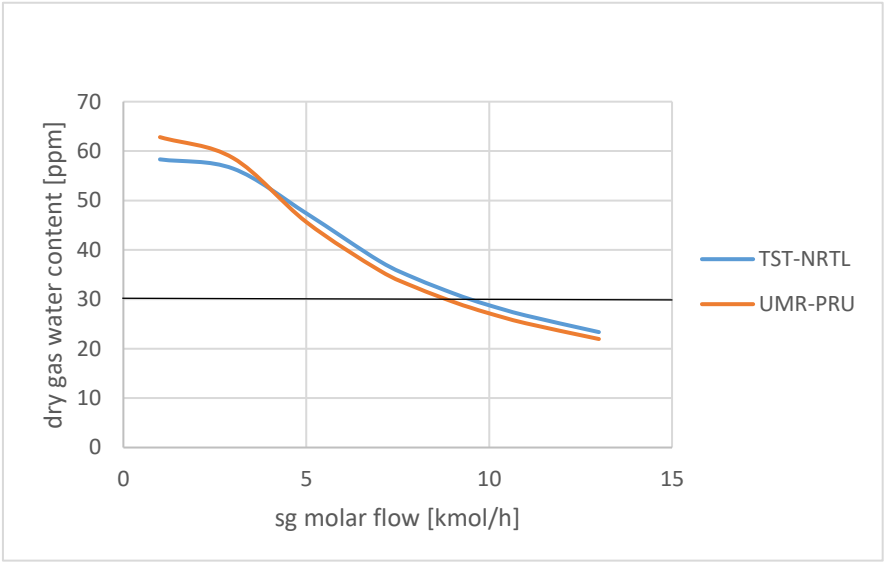

Figure 3.2 Effect of the stripping gas rate on the dry gas water content with the UMR-PRU and TST-NRTL models.

The decrease of the dry gas water content with the increase of the stripping gas rate can be explained as follows.

If a pseudo-binary ideal solution is assumed, then the water content is related to its partial pressure through eq. 3.1.

$$x_{water} = \frac{y_{H_2O}P}{P^s_{H_2O}} \quad \text{(Eq. 3.1)}$$

$$P \sim \sum_i y_i P = (y_{TEG}P) + (y_{H_2O}P) \quad \text{(Eq. 3.2)}$$

The term $(y_{TEG}P)$ is negligible compared to the other term of eq.3.2, due to the extremely low volatility of TEG. So, the insertion of stripping gas, results in the relationship presented in eq. 3.3.

$$P \sim \sum_i y_i P = (y_{H_2O}P) + (y_{sg}P) \quad \text{(Eq. 3.3)}$$

Since the pressure (P) of the column is constant, the partial pressure of water decreases, with the insertion of stripping gas. This corresponds to lower water content in the gas, as it is shown by eq. 3.1.

In figure 3.3 the trend of the lean TEG molar flow with the stripping gas rate is presented. Both models predict a descending trend of the lean TEG circulation rate with the increase of stripping gas rate and actually similar, with the exception of the very low values of the latter. Actually, this is the expected trend, since the lean TEG purity increases and thus the absorbing ability increases, leading to a decrease in the required amount of TEG.

Another parameter of importance to check during the sensitivity analysis is the effect on the required duties. As it is explained in section 2.4 where the simulation environment has been described, in the specific simulation, we considered two glycol/glycol heat exchangers, two glycol pumps and the glycol cooler. In addition to the abovementioned units, we should also considered the condenser and reboiler duties required in the distillation column, which has been used to simulate the Regenerator.

Figure 3.4 shows the effect of the stripping gas rate on the reboiler duty. Small differences have been observed with both considered models, for all the duties with the increase of stripping gas rate. It has been, also, observed that there is a difference between the duties calculated with TST-NRTL and UMR-PRU, which is attributed to the different pure TEG heat capacity calculated with the two models as it will be shown in section 3.5. Actually, UMR-PRU better predicts the aqueous TEG heat capacity compared to TST-NRTL and as such, the duties calculated with the first are considered closer to the actual case. [2] In the case of the reboiler duty, the increase in stripping gas rate, results in higher quantities needed to be heated up in the bottom of the column and thus increased reboiler duty. From the results of Tables 3.2 and 3.3 it is also observed that UMR-PRU systematically yields higher TEG loss compared to TST-NRTL. This is actually an outcome of the solubility of TEG in methane, which is higher for UMR-PRU and closer to the experimental data. [2]

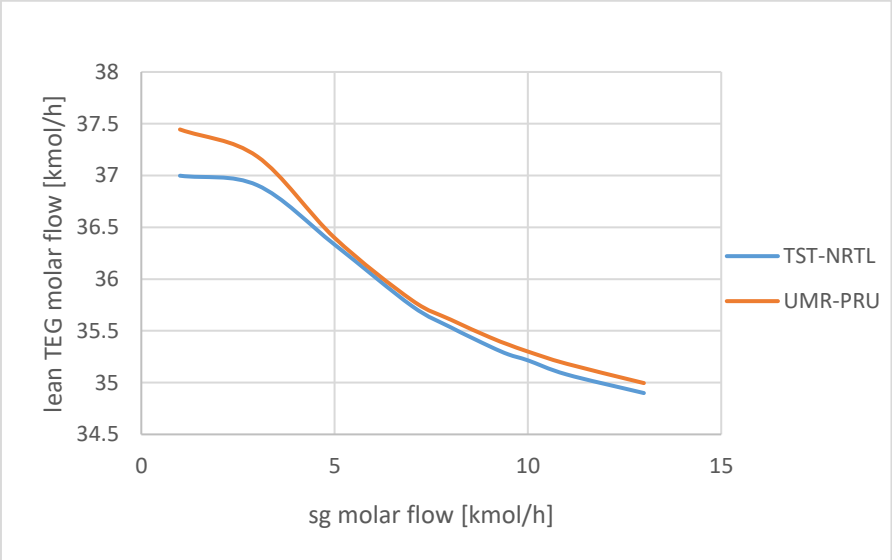

Figure 3. 3 Effect of the stripping gas rate on the lean TEG molar flow with the TST-NRTL and the UMR-PRU models.

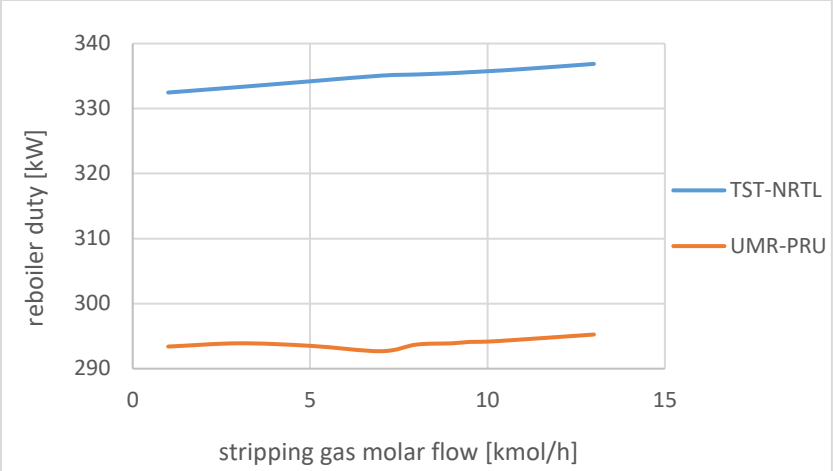

Figure 3.4 Effect of the stripping gas rate on the reboiler duty with the TST-NRTL and the UMR-PRU models.

Table 3 .2 Results of the analysis after variations of the stripping gas molar flow (TST/NRTL model)

sg molar flow [kmol/h]	lean TEG purity [wt]	lean TEG molar flow [kmol/h]	dry gas water content [ppm]	TEG loss [kmol/h]	heater duty [kW]	reboiler duty [kW]	cooler duty [kW]	pump 1 duty [kW]	pump 2 duty [kW]
1	0.9879	37.0	58	0.0003	0.91	332	209	0.53	9.3
3	0.9883	36.9	56	0.0011	1.47	333	209	0.53	9.3
5	0.9903	36.3	47	0.0019	2.08	333	209	0.53	9.3
7	0.9923	35.7	37	0.0026	2.76	335	209	0.53	9.3
8	0.9930	35.5	34	0.0030	3.10	335	209	0.53	9.2
9	0.9936	35.3	31	0.0034	3.43	335	209	0.52	9.2
9.5	0.9939	35.2	29	0.0036	3.59	335	210	0.52	9.2
10	0.9941	35.2	28	0.0038	3.76	335	210	0.52	9.2
11	0.9945	35.0	26	0.0042	4.08	336	210	0.52	9.2
13	0.9952	34.9	23	0.0050	4.72	336	210	0.52	9.2

Table 3. 3 Results of the analysis after variations of the stripping gas molar flow (UMR-PRU model)

sg molar flow [kmol/h]	lean TEG purity [wt]	lean TEG molar flow [kmol/h]	dry gas water content [ppm]	TEG loss [kmol/h]	heater duty [kW]	reboiler duty [kW]	cooler duty [kW]	pump 1 duty [kW]	pump 2 duty [kW]
1	0.9868	37.4	62	0.0014	0.96	293	209	0.54	9.7
3	0.9877	37.2	58	0.0026	1.48	293	209	0.54	9.7
5	0.9904	36.4	45	0.0039	2.11	293	209	0.54	9.7
7	0.9924	35.8	35	0.0051	2.77	293	209	0.54	9.7
8	0.9932	35.6	32	0.0057	3.10	293	209	0.54	9.7
9	0.9938	35.4	29	0.0064	3.43	293	209	0.54	9.7
9.5	0.9940	35.3	28	0.0067	3.59	294	209	0.54	9.7
10	0.9942	35.3	27	0.0070	3.75	294	209	0.54	9.7
11	0.9947	35.1	25	0.0076	4.06	294	209	0.54	9.7
13	0.9953	35.0	21	0.0088	4.68	295	209	0.54	9.7

3.2 Variation of the reboiler temperature

Next the variation of the reboiler temperature is examined. In particular, since the range of temperature considered to do the analysis is small, no significant effects have been expected. The reason why this small range of temperature has been analyzed is the limitation of the TEG degradation temperature. Since there is a range of temperature in the literature for this property, ranging from about 202 to 206^{o}C, this analysis is performed in a temperature range starting at about 200^{o}C.

Figure 3.5 shows the trend of the lean TEG purity after variations of the reboiler temperature. As it has been expected, there is an increase of the lean TEG purity with the increase of reboiler temperature with both the models. A slight difference in the

lean TEG purity is observed between UMR-PRU and TST-NRTL. This is attributed to the different performance of the two models in the vapor – liquid equilibrium of natural gas components with water and TEG, as mentioned in the previous case.

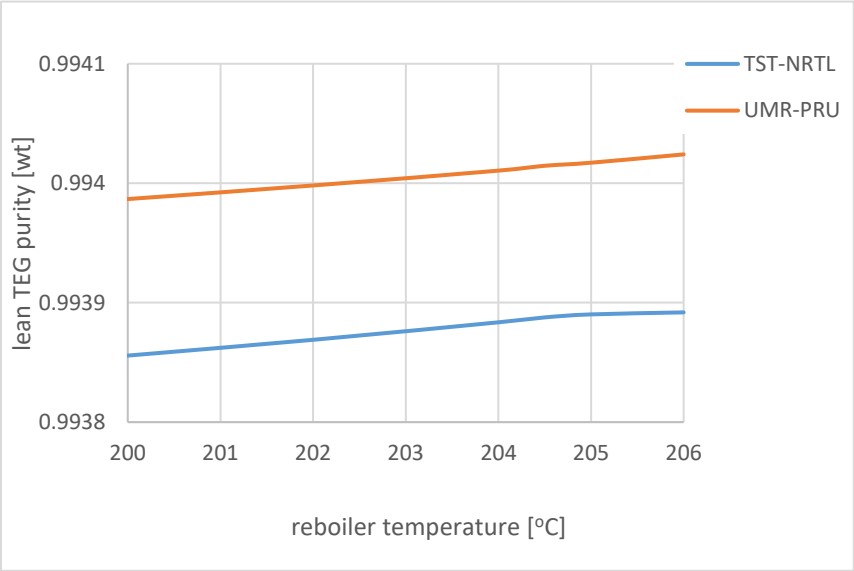

Figure 3.5 Effect of the reboiler temperature on the lean TEG purity with the TST-NRTL and the UMR-PRU models.

Figure 3.6 shows the trend of the dry gas water content after variations of the reboiler temperature. As expected from the results in the purity of the lean TEG, the dry gas water content decreases with the increase of the reboiler temperature, due to the higher absorbing capacity of the solvent. If the performance of the models in meeting the required specification of 30 ppm of water in the dry gas is examined, it is observed that this specification has been met for the whole analysis with both the models. In particular, UMR-PRU model leads to a lower water content in the dry gas stream due to the higher purity of the recycled lean TEG, compared to TST-NRTL model.

Another parameter of importance to check during the sensitivity analysis is the effect on the required duties. Figure 3.7 shows the effect of the reboiler temperature on the reboiler duty. Great differences have been observed with both considered models, for the reboiler and cooler duties with the increase of reboiler temperature, while the influence of the parameter under consideration on the other duties is quite negligible.

It has been also observed that there is a difference between the duties calculated with TST-NRTL and UMR-PRU, which is attributed to the different pure TEG heat capacity calculated with the two models as mentioned in the previous section. In the case of the reboiler duty which trend is shown in Figure 3.7, the increase in reboiler temperature, results in higher quantity of energy needed to reach these temperatures in the bottom of the distillation column and thus increased reboiler duty. For what concerns the cooler duty, since the ΔT between contactor and regenerator increases due to the increase of the reboiler temperature, higher amounts of energy are required from the recycled lean TEG stream to reach the contactor operating conditions, as it is shown in Figure 3.8.

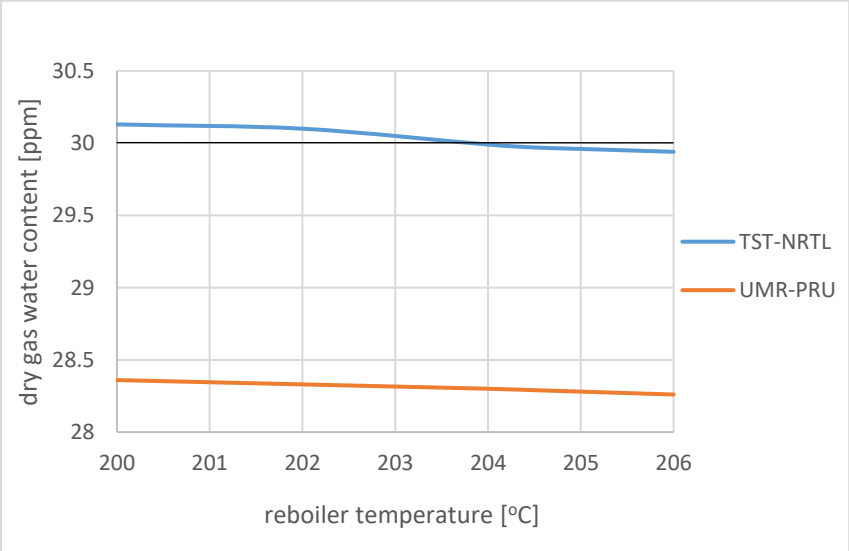

Figure 3.6 Effect of the reboiler temperature on the dry gas water content with the TST-NRTL and the UMR-PRU models.

The detailed results of the sensitivity analysis in terms of reboiler temperature are given in Tables A.1 and A.2 in the Appendix.

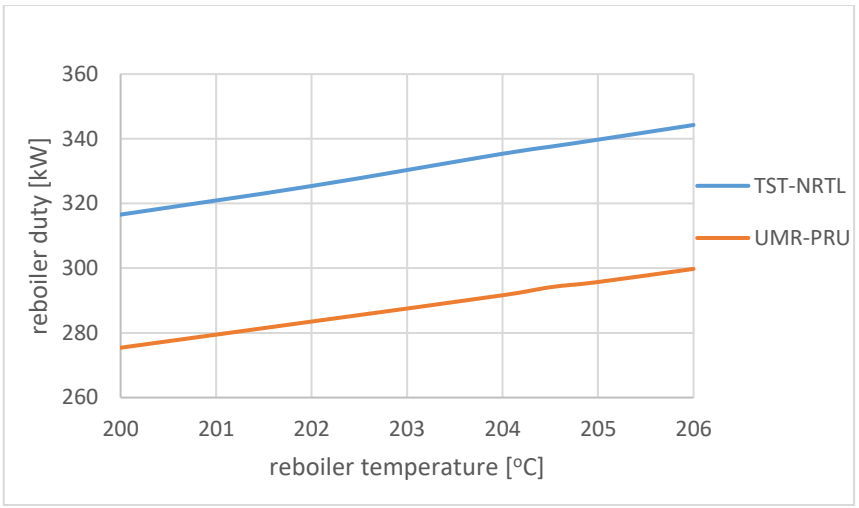

Figure 3.7 Effect of the reboiler temperature on the reboiler duty with the TST-NRTL and the UMR-PRU models.

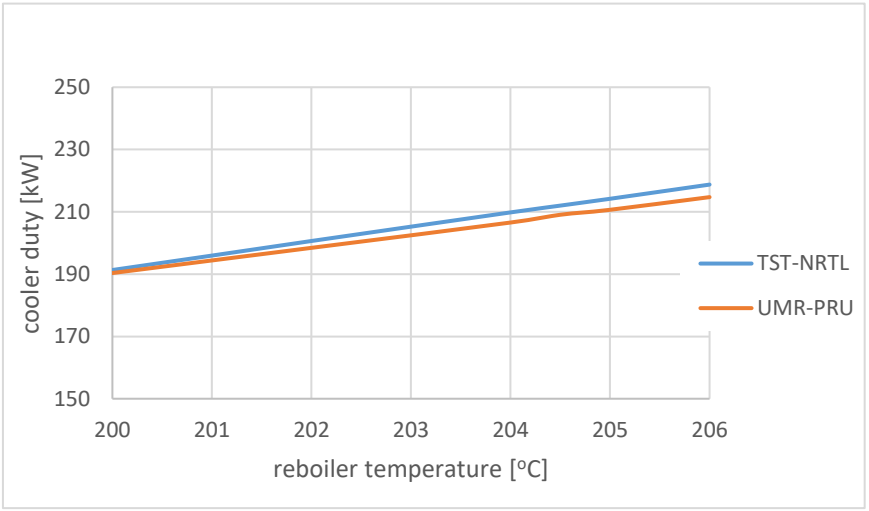

Figure 3.8 Effect of the reboiler temperature on the cooler duty with the TST-NRTL and the UMR-PRU models.

3.3 Variation of the reboiler pressure

The sensitivity analysis which concerns the variation of the reboiler pressure has been made without the use of stripping gas, since operation under vacuum conditions is an alternative procedure of increasing lean TEG purity compared to stripping gas. Furthermore, since the operating pressure changes, the specified condenser temperature

should also change accordingly, in order to satisfy the equilibrium conditions. The specified temperatures for each case are presented in Tables A.3 and A.4 in Appendix.

Figure 3.9 shows the trend of the lean TEG purity after variations of the reboiler pressure. In particular, there is a decrease of the lean TEG purity with the increase of reboiler pressure with both the models, as expected since the analysis has been conducted under vacuum conditions. A slight difference in the lean TEG purity is observed for pressures close to the atmospheric one between UMR-PRU and TST-NRTL. This is attributed to the different performance of the two models in the vapor – liquid equilibrium of natural gas components with water and TEG.

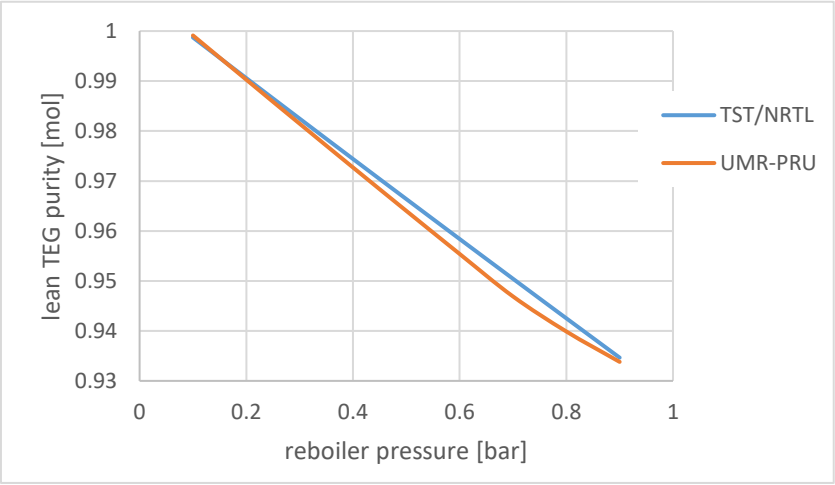

Figure 3. 9 Effect of the reboiler pressure on the lean TEG purity with the TST-NRTL and the UMR-PRU models.

Figure 3.10 shows the trend of the dry gas water content after variations of the reboiler pressure. As expected from the results in the purity of the lean TEG, the dry gas water content increases with the increase of the reboiler pressure, due to the lower absorbing capacity of the solvent. If the performance of the models in meeting the required specification of 30 ppm of water in the dry gas is examined, it is observed that this specification is met for pressures under approximately 0.75 bar with both models. In particular, UMR-PRU model leads to a lower water content in the dry gas stream for the same pressure, due to the higher purity of the recycled lean TEG, compared to TST-NRTL model.

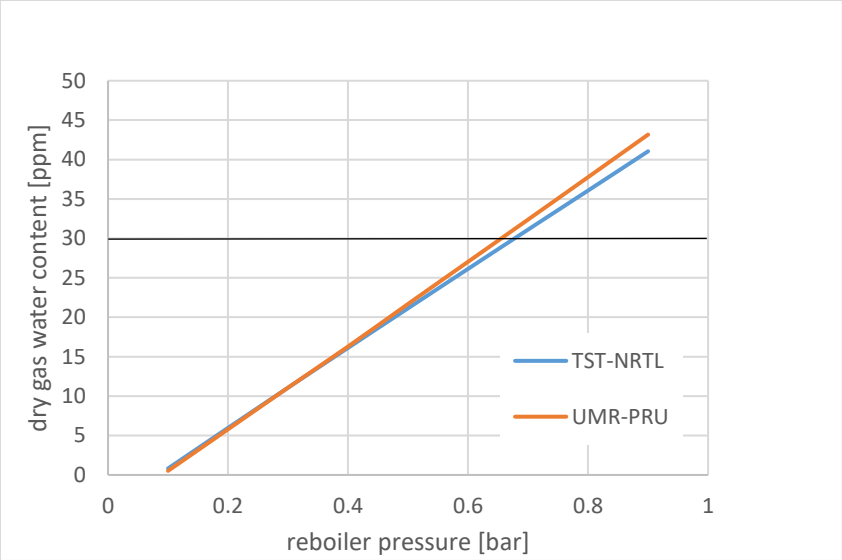

Figure 3.10 Effect of the reboiler pressure on the dry gas water content with the TST-NRTL and the UMR-PRU models.

Another parameter checked during the sensitivity analysis is the effect on the required duties. Slight differences have been observed with both considered models, for the duties required by the process. The highest effect is observed on the reboiler duty, as it is shown in Figure 3.11. As in the previous cases, there is a difference between the duties calculated with TST-NRTL and UMR-PRU, which is attributed to the different pure TEG heat capacity calculated with the two models. The increase in reboiler pressure results in lower reboiler duty, since the separation is enhanced at lower pressure. The detailed results of the sensitivity analysis in terms of reboiler pressure are given in Tables A.3 and A.4 in Appendix.

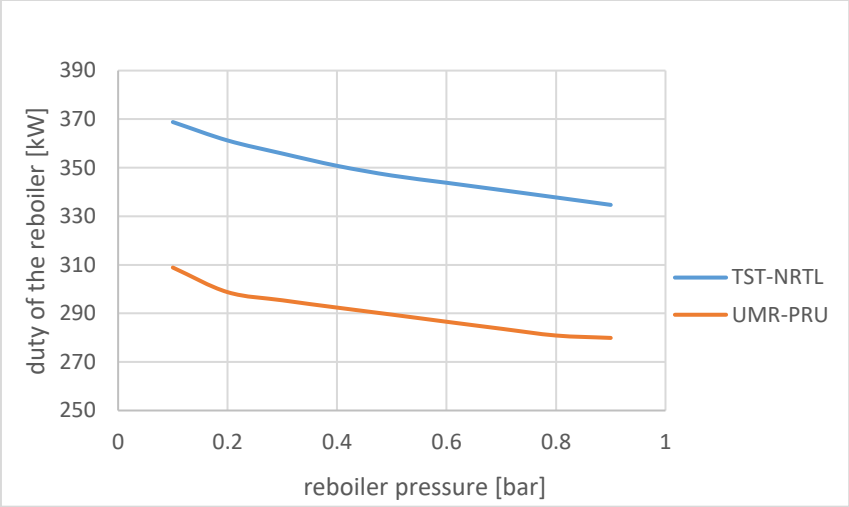

Figure 3.11 Effect of the reboiler pressure on the reboiler duty with the TST-NRTL and the UMR-PRU models.

3.4 Variation of the flash drum temperature

The following sensitivity analysis concerns the variation of the flash drum temperature. The scope of inserting this piece of equipment is to remove the diluted hydrocarbons in the rich TEG stream prior to the Regeneration.

Figure 3.12 shows the trend of the lean TEG purity after variations of the flash drum temperature. As it has been expected there is an increase of the lean TEG purity with the increase of flash drum temperature with both the models, due to the removal of some water in the flash along with the hydrocarbons. A slight difference in the lean TEG purity is observed between UMR-PRU and TST-NRTL, as defined by their respective VLE results.

Figure 3.13 shows the trend of the dry gas water content after variations of the flash drum temperature. As expected from the results in the purity of the lean TEG, the dry gas water content decreases with the increase of the flash drum temperature, due to the higher amount of water which exits the plant with the flash gas. If the performance of the models in meeting the required specification of about 30 ppm of water in the dry gas is examined, it is observed that this specification has been met for the whole analysis with both examined models. In particular, UMR-PRU model leads to a lower

water content in the dry gas stream due to the higher purity of the recycled lean TEG, compared to TST-NRTL model.

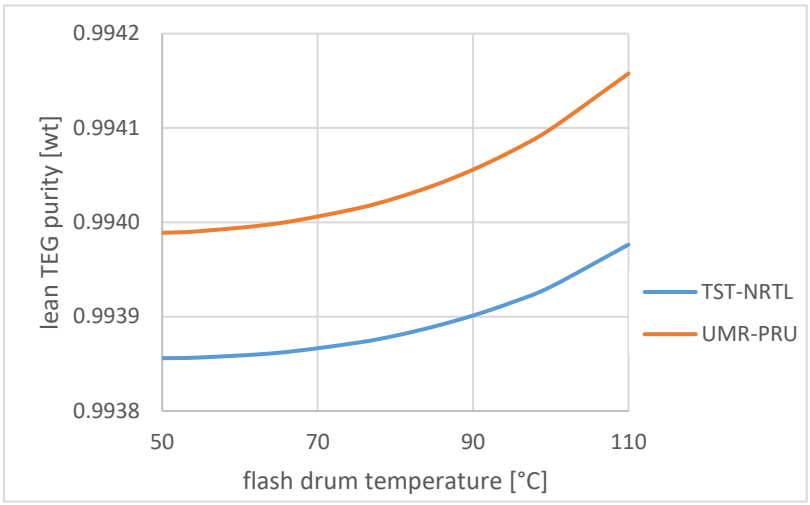

Figure 3.12 Effect of the flash drum temperature on the lean TEG purity with the TST-NRTL and the UMR-PRU models.

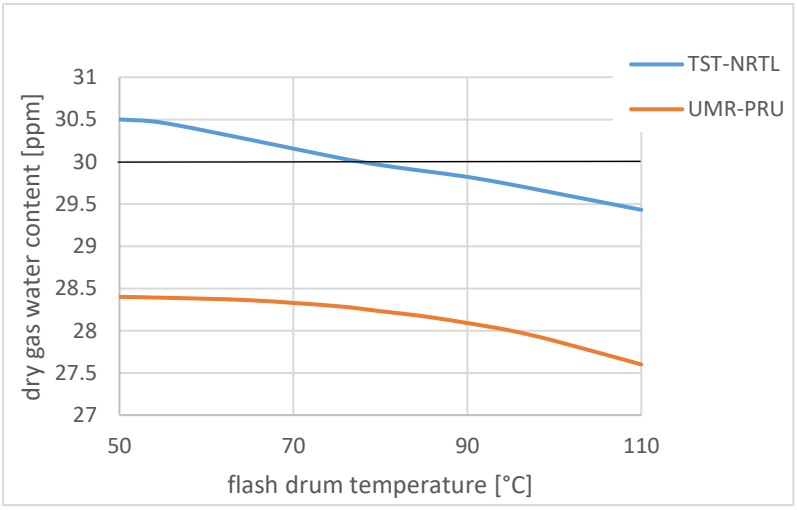

Figure 3.13 Effect of the flash drum temperature on the dry gas water content with the TST-NRTL and the UMR-PRU models.

Not significant differences have been observed with both considered models, for the duties required by the process with the increase of flash drum temperature. Figure 3.14 shows the effect of the flash drum temperature on the reboiler duty. Since the influence of the parameter analyzed is negligible, the trend is almost constant.

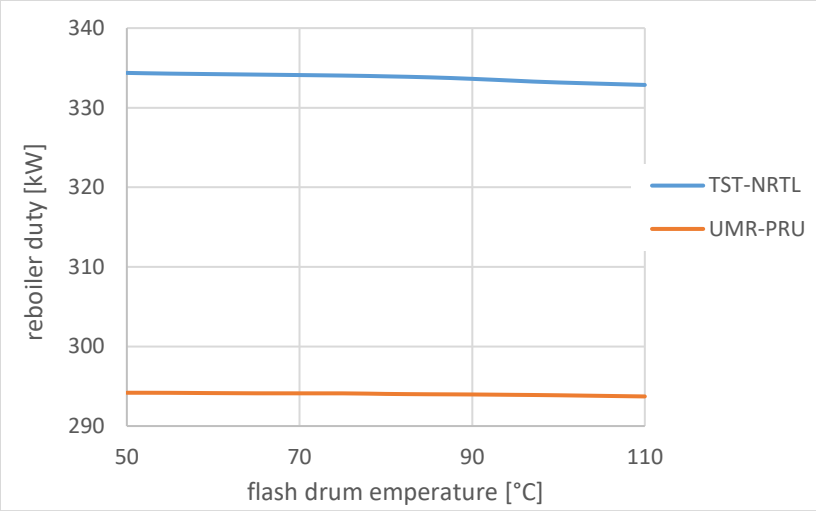

Figure 3.14 Effect of the flash drum temperature on the reboiler duty with the TST-NRTL and the UMR-PRU models.

Figure 3.15 shows an almost constant trend for the flash gas hydrocarbons content. However, there is a difference on this content between the two models, since a higher amount of hydrocarbons is vented off with UMR-PRU, due to a higher solubility of hydrocarbons in the gas phase calculated with UMR-PRU model compared to TST-NRTL. [2] For what concerns water and TEG content of the flash gas, as shown in Figure 3.16 and Figure 3.17 respectively, there is an increase of both these contents, which means higher purities of the recycled lean TEG, but also higher amount of TEG loss.

The detailed results of the sensitivity analysis in terms of flash drum temperature are given in Tables A.5 and A.6.

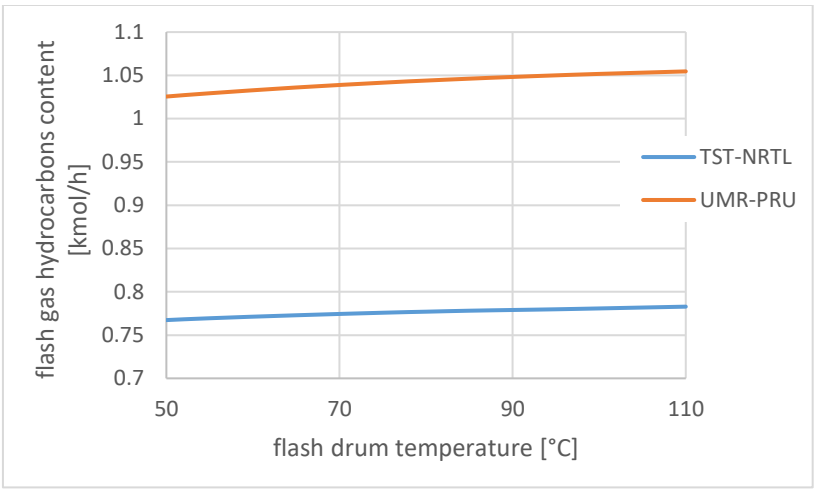

Figure 3 .15 Effect of the flash drum temperature on the flash gas hydrocarbons content with the TST-NRTL and the UMR-PRU models.

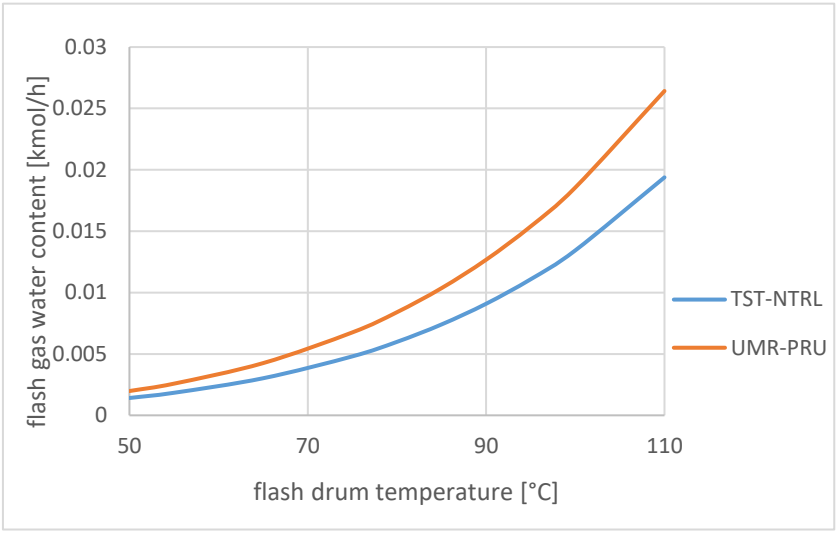

Figure 3 .16 Effect of the flash drum temperature on the flash gas water content with the TST-NRTL and the UMR-PRU models.

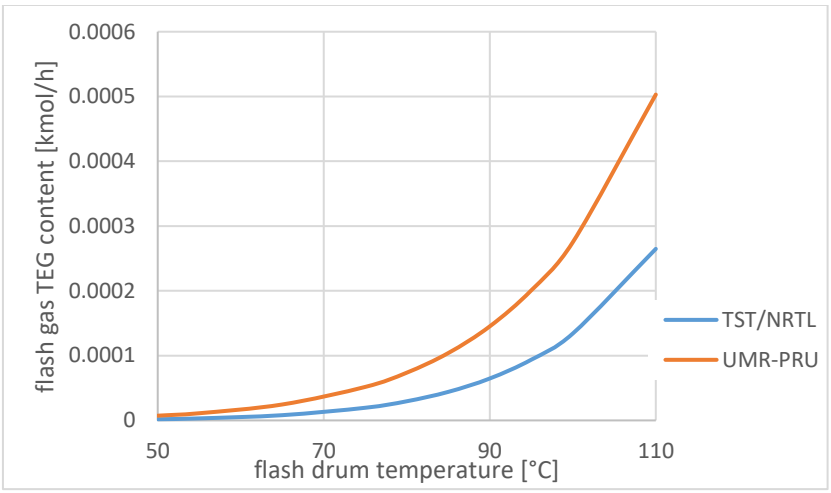

Figure 3 .17 Effect of the flash drum temperature on the flash gas TEG content with the TST-NRTL and the UMR-PRU models.

3.5 Variation of the input regenerator temperature

The following sensitivity analysis concerns the variation of the temperature of the rich TEG stream entering the distillation column. This parameter has been varied to evaluate its impact on the whole process and, especially, on the regeneration section.

Figure 3.18 shows the trend of the lean TEG purity after variations of the input regenerator temperature. As it has been expected, there is an increase of the lean TEG purity with the increase of flash drum temperature with both models. A slight difference in the lean TEG purity is observed between UMR-PRU and TST-NRTL, due to their difference in VLE.

Figure 3.19 shows the trend of the dry gas water content after variations of the flash drum temperature. As expected from the results in the purity of the lean TEG, the dry gas water content decreases with the increase of the flash drum temperature, due to the higher amount of water which exits the plant with the flash gas. If the performance of the models in meeting the required specification of about 30 ppm of water in the dry gas is examined, it is observed that this specification has been met for temperatures

higher than 127ºC for UMR-PRU model and for temperatures higher than 140ºC for TST-NRTL.

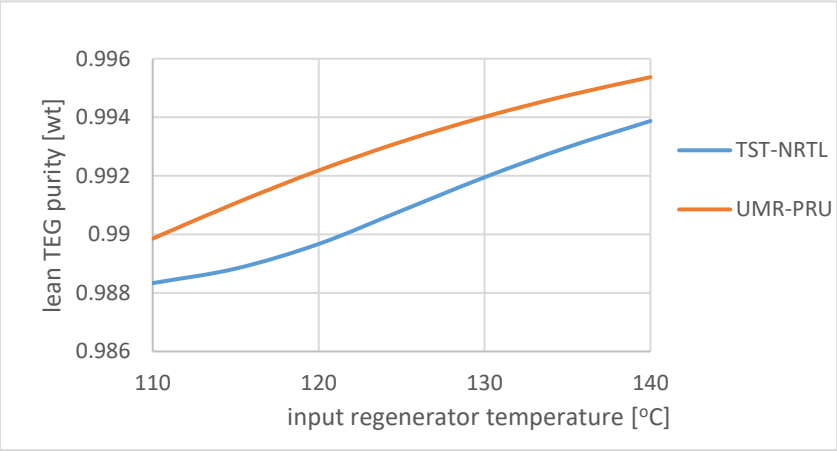

Figure 3.18 Effect of the input temperature of the rich TEG stream entering the regenerator on the lean TEG purity with the TST-NRTL and the UMR-PRU models.

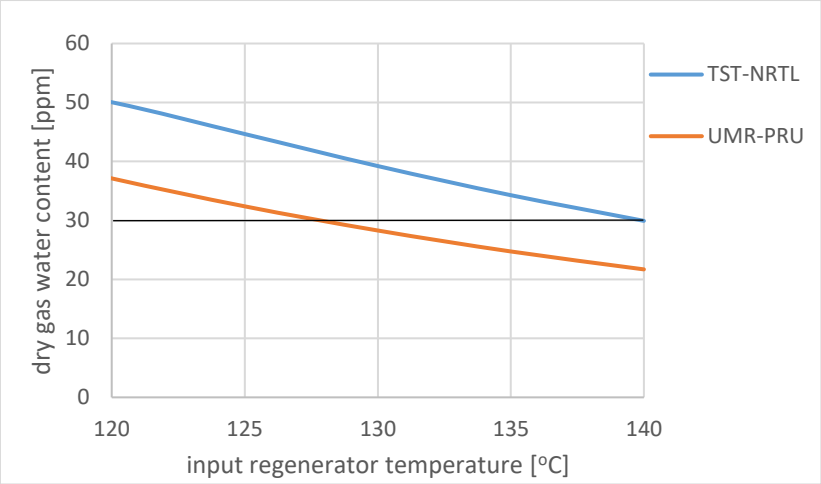

Figure 3.19 Effect of the input temperature of the rich TEG stream entering the regenerator on the dry gas water content with the TST-NRTL and the UMR-PRU models.

Another parameter of importance during the sensitivity analysis is the effect on the required duties. Figure 3.20 shows the effect of the input regenerator temperature on the reboiler duty. Great differences has been observed with the both considered models, for all the duties with the increase of stripping rate. The increase of the temperature of

the rich TEG stream entering the regenerator leads to a significant decrease of the reboiler duty.

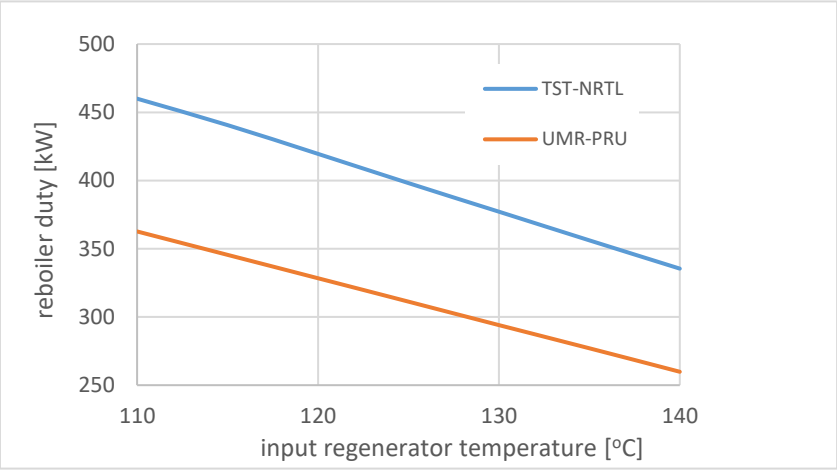

Figure 3 .20 Effect of the input temperature of the rich TEG stream entering the regenerator on the reboiler duty with the TST-NRTL and the UMR-PRU models.

It has been also observed that there is a difference between the duties calculated with TST-NRTL and UMR-PRU, which is attributed to the different pure TEG heat capacity calculated with the two models. In particular, Figure 3.21 shows the trend of the heat required by the stream entering the reboiler in order to reach the saturation conditions. Since UMR-PRU model predicts lower heat capacities compared to TST-NRTL, as it is shown in Figure 3.21, the reboiler duty required by the simulation with this model is lower. Actually, as it has been shown in Ref. [2] the heat capacity of aqueous TEG mixture with UMR-PRU is better compared to TST-NRTL and as such, it is expected that the calculations will be closer to the actual process data.

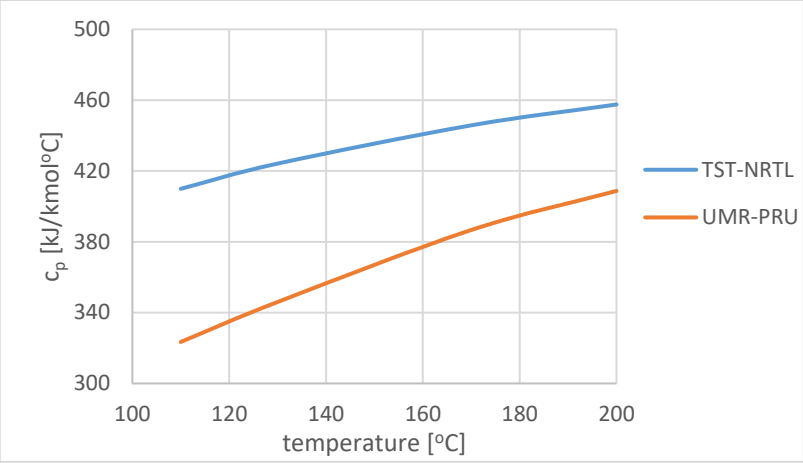

Figure 3.21: Effect of the temperature on the heat capacity for TST-NRTL and UMR-PRU models

An increase of the input regenerator temperature leads also to a decrease of the cooler duty, as it is shown in Figure 3.22. In fact, since a higher amount of heat passes from the lean TEG stream to the rich TEG into the glycol/glycol heat exchanger with the increase of the temperature, higher cooler duties are required by the recycled TEG in order to reach the contactor operating conditions.

The total TEG loss and the amount of TEG vented off with the dry gas, flash gas and vapor streams have been also analyzed. Figure 3.23 shows that the highest amount of glycol exits the plant with the vapor stream out of the regenerator but, no significant variations occur due to the increase of the input temperature to the regenerator.

The detailed results of the sensitivity analysis in terms of input this variable are given in Tables A.7 and A.8.

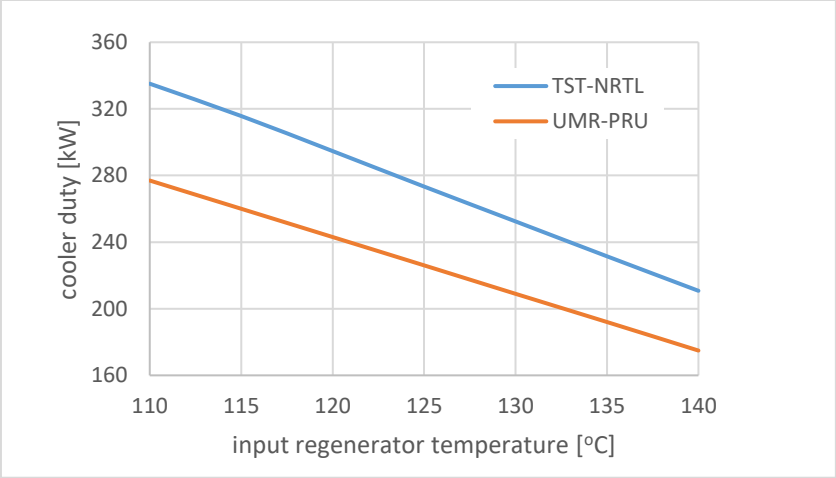

Figure 3.22 Effect of the input temperature of the rich TEG stream entering the regenerator on the cooler duty with the TST-NRTL and the UMR-PRU models.

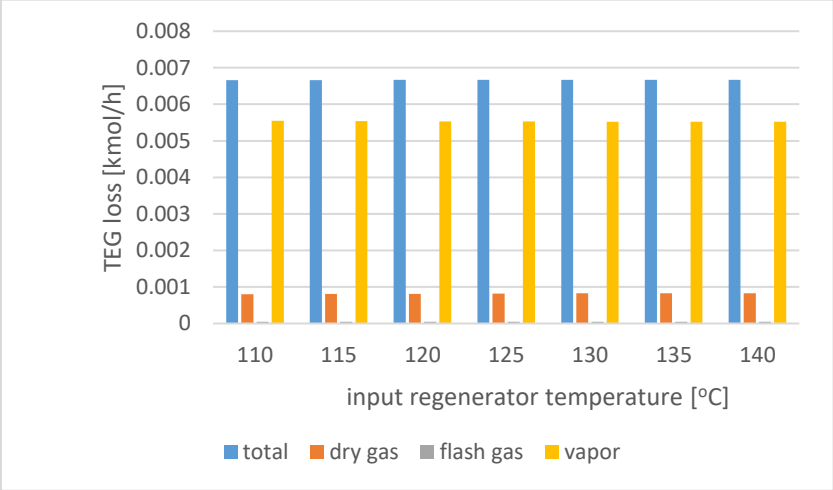

Figure 3.23 Effect of the input temperature of the rich TEG stream entering the regenerator on the TEG loss with the TST-NRTL and the UMR-PRU models.

3.6 Variation of the contactor temperature

The lowest contactor temperature examined in this analysis, is limited by the hydrates formation. To this purpose, the hydrate analysis method of van der Waals and Platteux which is incorporated in HYSYS is used to define the lowest temperature at the examined pressure and wet gas stream where hydrates would not form. Based on

the previous, a temperature of about 12°C has been calculated. As a result, temperature higher than 12°C has been considered for the contactor temperature.

Figure 3.24 shows the trend of the lean TEG purity after variations of the contactor temperature. There is a slight increase of the lean TEG purity with the increase of contactor temperature with both the models. This result occurs because, since a lower amount of water exits the bottom of the contactor due to a worst absorption process which occurs with higher temperatures, this lower water content is found again in the recycled lean TEG stream.

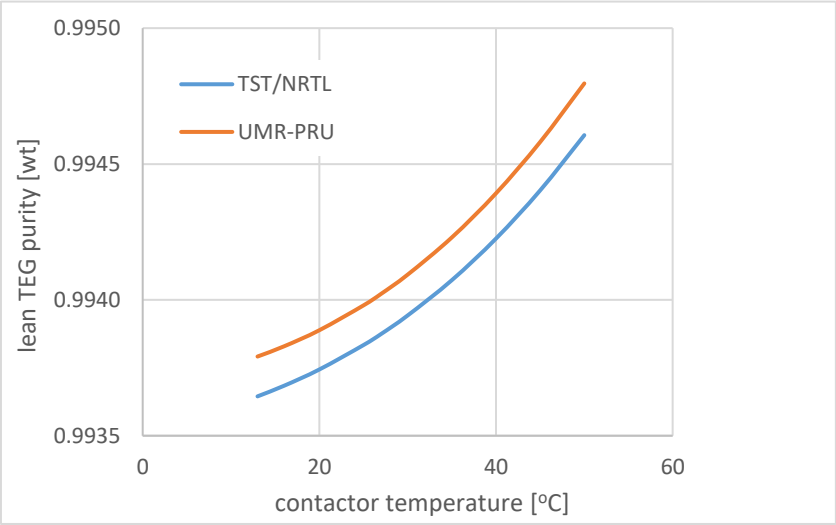

Figure 3 .24 Effect of the contactor temperature on the lean TEG purity with the TST-NRTL and the UMR-PRU models.

Figure 3.25 shows the trend of the dry gas water content after variations of the contactor temperature. The dry gas water content increases with the increase of the contactor temperature, due to the worst absorption process which occurs at higher temperatures. If the performance of the models in meeting the required specification of about 30 ppm of water in the dry gas is examined, it is observed that this specification has been met for temperatures lower that 27°C with both models. Actually, with the increase of temperature, increases the water solubility in vapor phase and as such, the water content is increased.

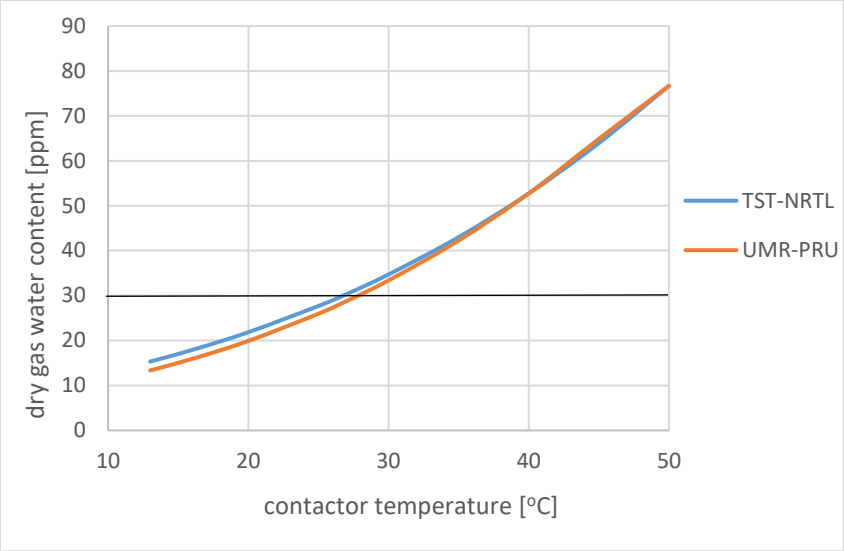

Figure 3.25 Effect of the contactor temperature on the dry gas water content with the TST-NRTL and the UMR-PRU models.

For what concerns the effect on the required duties, the variation of the contactor temperature has a great influence only on the cooler duty, as presented in Figure 3.26. Instead, the reboiler duty, shown in Figure 3.27, is almost constant for both models. The trend of the cooler duty can be explained by considering that the lean TEG stream transfers a lower amount of heat to the rich TEG stream in the glycol/glycol heat exchanger due to the higher temperature of the liquid stream exiting the contactor. For this reason, the recycled lean TEG needs a higher amount of energy to reach the contactor operating conditions.

A difference between the two models occurs in the rich TEG hydrocarbons content, as it is shown in Figure 3.28. Actually, the UMR-PRU model results to a higher amount of hydrocarbons in the glycol-rich stream exiting the contactor. The increase of temperature, leads to a decrease of the hydrocarbon content for the UMR-PRU model. For the TST-NRTL, on the other hand, there is no remarkable difference, probably due to the very low solubilities encountered.

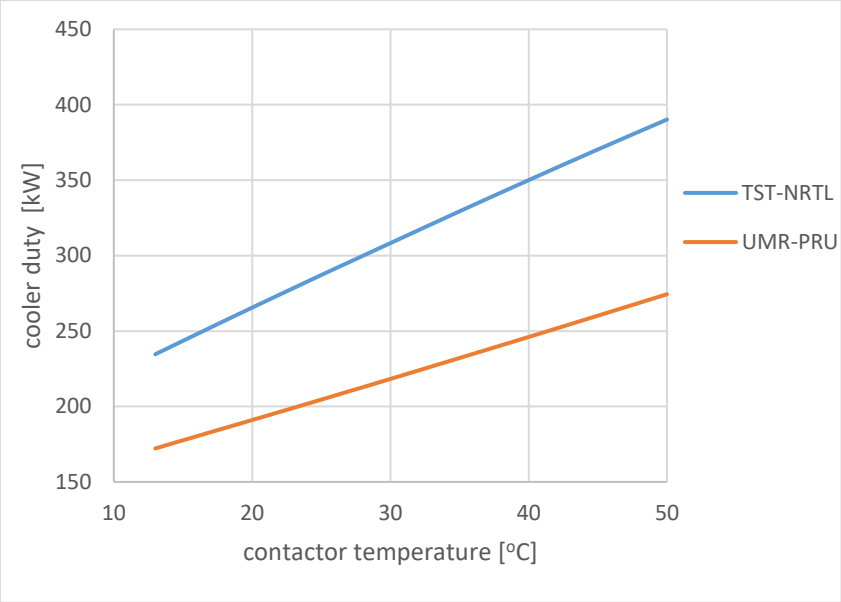

Figure 3.26 Effect of the contactor temperature on the cooler duty with the TST-NRTL and the UMR-PRU models.

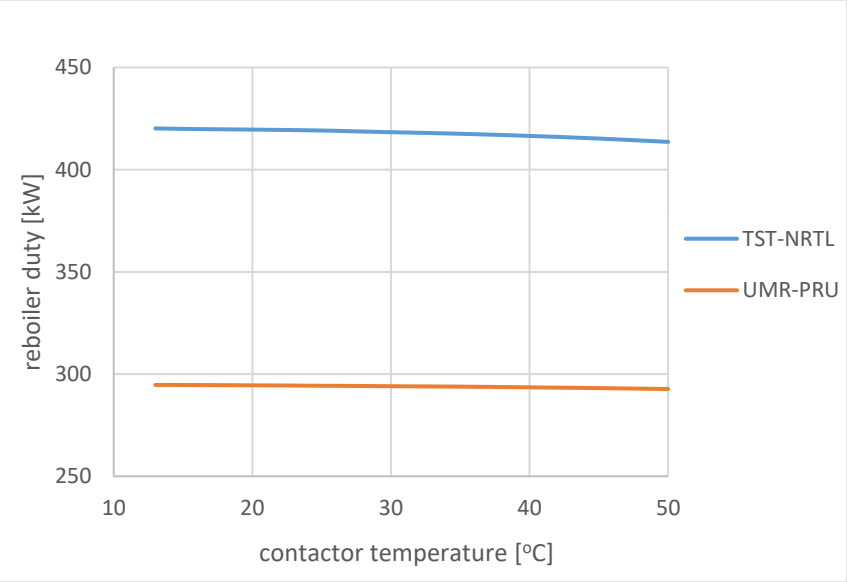

Figure 3.27 Effect of the contactor temperature on the reboiler duty with the TST-NRTL and the UMR-PRU models.

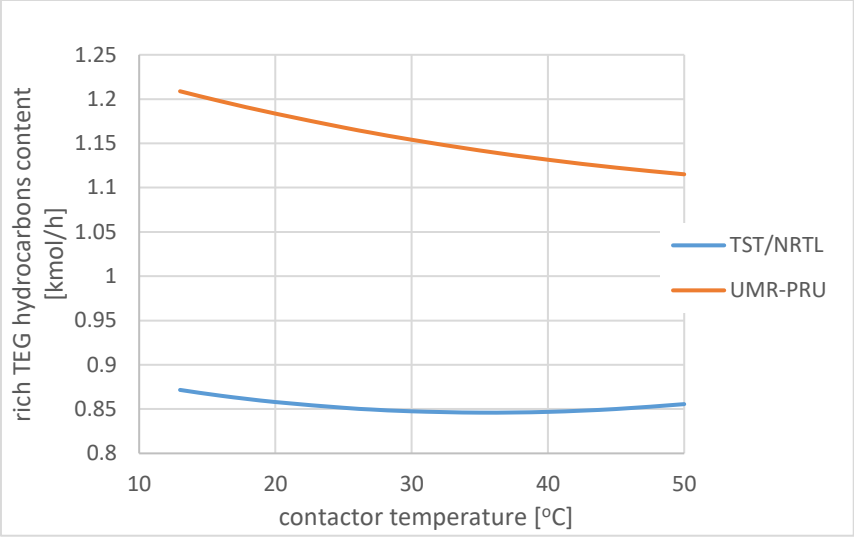

Figure 3. 28 Effect of the contactor temperature on the rich TEG hydrocarbons content with the TST-NRTL and the UMR-PRU models.

Furthermore, there is an increase of the TEG loss in the dry gas stream, with the increase of the contactor temperature. In particular, most of TEG is vented off with the vapor stream out of the regenerator, but the highest influence of the variation of the contactor temperature is on the dry gas TEG content, as it shown in Figure 3.29.

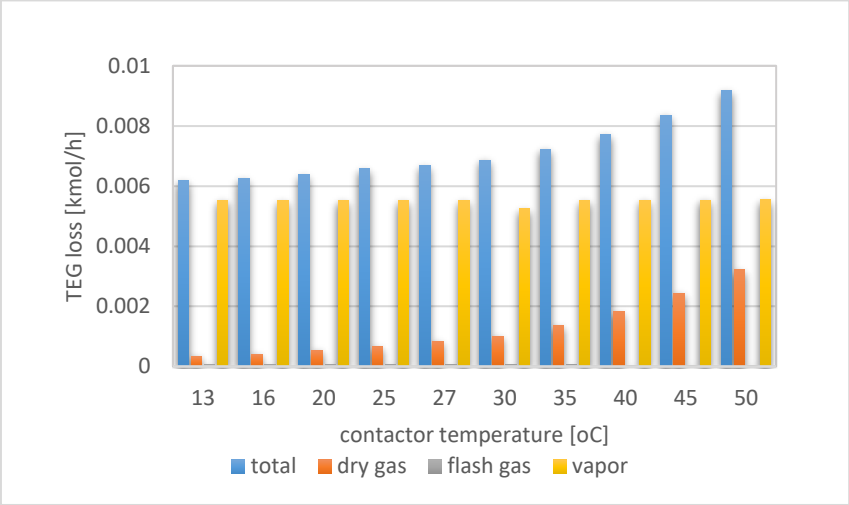

Figure 3.29 Effect of the contactor temperature on the TEG loss with the TST-NRTL and the UMR-PRU models.

The detailed results of the sensitivity analysis in terms of contactor temperature are given in Tables A.9 and A.10.

3.7 Variation of the contactor pressure

In this sensitivity analysis, the effect of the variation of the contactor pressure has been analyzed. Figure 3.30 shows the trend of the dry gas water content after variations of the contactor pressure. The dry gas water content increases with the increase of the flash drum pressure due to two different reasons: one is that at higher pressures the solubility of water in the gas phase increases; the second is that the contactor pressure influences the absorption capacity of TEG. Therefore, the increase of contactor pressure leads to a lower solubility of water in the gas phase. If the performance of the models in meeting the required specification of about 30 ppm of water in the dry gas is examined, it is observed that UMR-PRU model requires slight higher pressures compared to TST-NRTL.

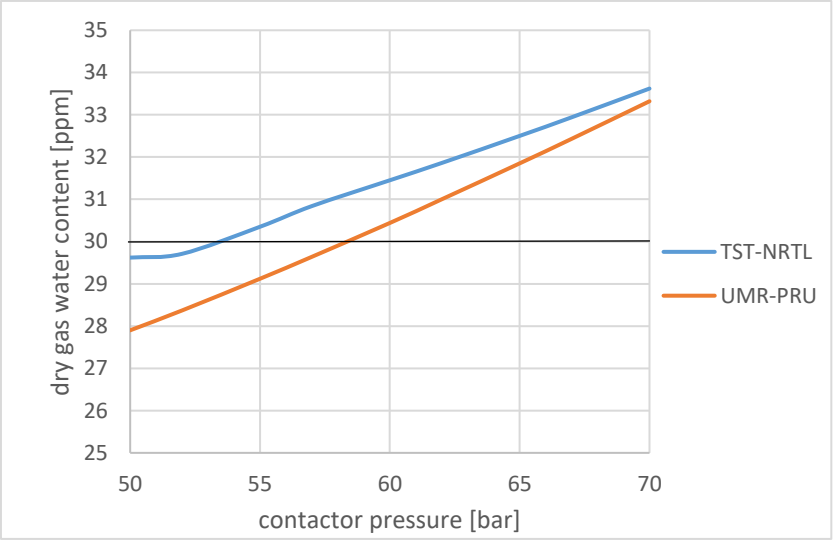

Figure 3. 30 Effect of the contactor pressure on the dry gas water content with the TST-NRTL and the UMR-PRU models.

For what concerns the effect on the required duties, the variation of the contactor temperature has a great influence only on the cooler duty shown in Figure 3.31, instead the reboiler duty shown in Figure 3.32 is almost constant for both models.

Figure 3.33 shows the effect of the contactor pressure on the rich TEG hydrocarbons content. An increase of the contactor pressure leads to an increase of this content for both models. However, there is a difference between the two trends due to the different solubility of hydrocarbons in the rich TEG stream. In particular, a higher amount of these components exits the bottom of the contactor with UMR-PRU model due to their higher solubility in the rich TEG, compared to TST-NRTL, as shown in Figure 3.33.

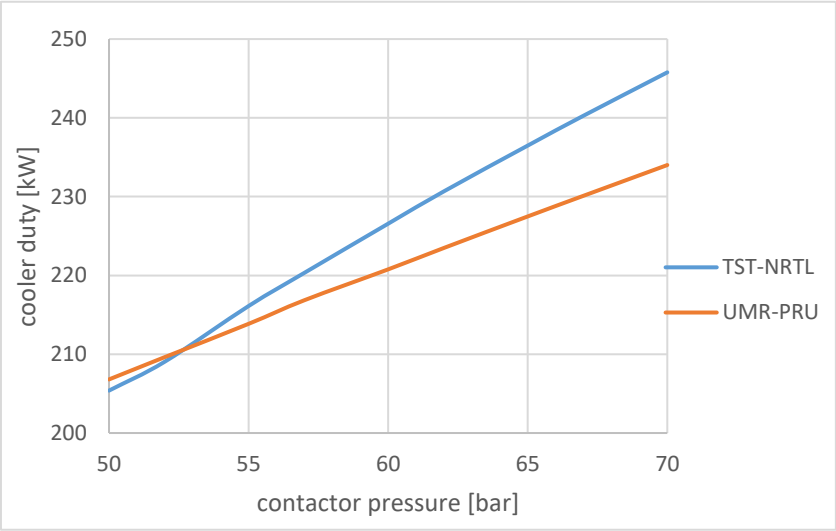

Figure 3 .31 Effect of the contactor pressure on the cooler duty with the TST-NRTL and the UMR-PRU models.

The detailed results of the sensitivity analysis in terms of contactor pressure are given in Tables A.11 and A.12.

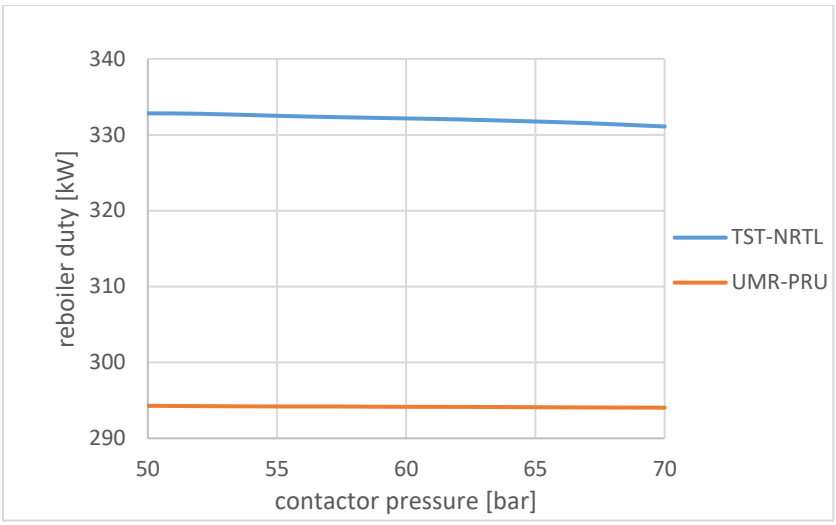

Figure 3.32 Effect of the contactor pressure on the reboiler duty with the TST-NRTL and the UMR-PRU models.

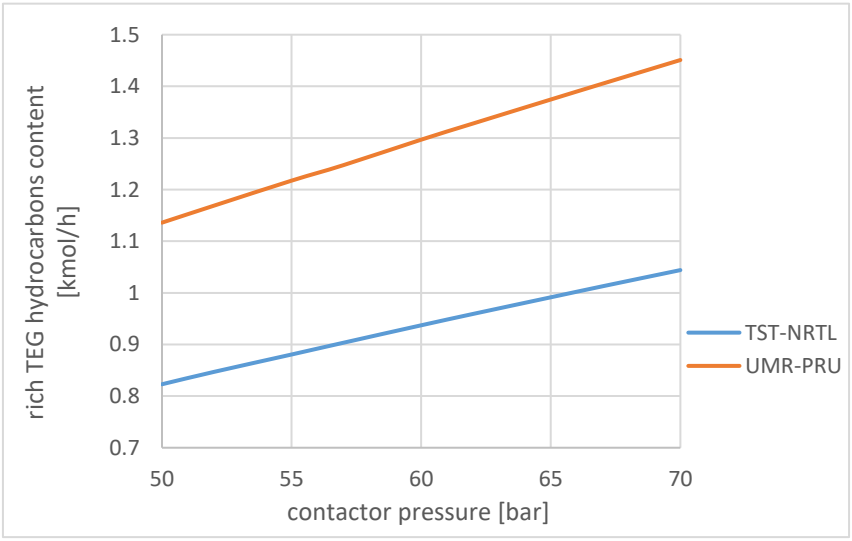

Figure 3.33 Effect of the contactor pressure on the rich TEG hydrocarbons content with the TST-NRTL and the UMR-PRU models.

3.8 Results of the sensitivity analysis

From the previous sensitivity analysis it possible to sum up the following results:

- the increase of the stripping gas molar flow leads to an increase of the lean TEG purity and a decrease of the lean TEG molar flow and of the dry gas water content.
- the increase of the reboiler temperature leads to an increase of both reboiler and cooler duties.
- the increase of the reboiler pressure leads to a decrease of both the lean TEG purity and the reboiler duty, and to an increase of the dry gas water content.
- the increase of the flash drum temperature leads to a decrease of the dry gas water content, with no significant impact on the required duties.
- the increase of the temperature of the stream entering the regenerator leads to a decrease of the dry gas water content, as well as to the reboiler and cooler duties.
- the increase of the contactor temperature leads to an increase of the dry gas water content and of the cooler duty.
- the increase of the contactor pressure leads to an increase of dry gas water content and of the cooler duty.

Following these results, an optimization of the operating variables of the process occurs, in terms of the required duties, by simultaneously changing the flash drum temperature and the temperature of the rich TEG stream entering the regenerator. A slight modification has been done also to the contactor pressure, since from the sensitivity analysis the result has been that lowering this pressure would result to a lower dry gas water content. To this purpose, the specification of 30 ppm as dry gas water content is considered, using the stripping gas rate as the independent variable.

The results of the optimized parameters for both models are reported on Table 3.4. In order to improve the whole process, the temperatures of the flash drum and of the stream entering the regenerator have been increased for both models, while the other parameters have been kept at the same values as in the base conditions.

Table 3. 4 Base and optimized operating conditions for TST-NRTL and UMR-PRU model

	base conditions (TST-NRTL and UMR-PRU)	optimized conditions (TST-NRTL)	optimized conditions (UMR-PRU)
reboiler temperature [^{o}C]	204.6	204.6	204.6
reboiler pressure [bar]	1.27	1.27	1.27
flash drum temperature [^{o}C]	75	100	90
input regenerator temperature [^{o}C]	130	137	137
contactor temperature [^{o}C]	27	27	27
contactor pressure [bar]	51.65	50	50

Table 3.5 shows the results of the simulation with base and optimized operating conditions for both models. The reported results show that in the optimized conditions a decrease of both reboiler and cooler duties is obtained with both examined models. Furthermore, this is achieved with the use of a lower amount of stripping gas rate. Actually, this corresponds to a 9% decrease for the required duties of TST-NRTL between the base and optimized conditions, while in the case of UMR-PRU this is about 8.2%. In terms of stripping gas rate, in the case of TST-NRTL a reduction of about 21% in stripping gas rate is obtained, while for UMR-PRU this equals 26%. If the results of the two different models in the same conditions (e.g. base scenario) are considered, UMR-PRU requires systematically lower reboiler duty compared to TST-NRTL. As it has been described in Section 3.5, this is attributed to the different calculation of the heat capacity of TEG.

Table 3.5 Simulation results with base and optimized operating conditions with TST-NRTL and UMR-PRU models

	base conditions		optimized conditions	
	TST/NRTL	UMR-PRU	TST/NRTL	UMR-PRU
stripping gas molar flow [kmol/h]	9.5	9.5	7.5	7
lean TEG purity [mol]	0.9517	0.9509	0.9523	0.9506
lean TEG purity [wt]	0.9939	0.9938	0.9940	0.9937
lean TEG molar flow [kmol/h]	35.1	35.3	35.2	35.5
dry gas water content [ppm]	29.93	29.52	29.54	29.8
dry gas TEG content [ppm]	1.65	3.60	1.65	3.40
TEG loss [kmol/h]	0.0040	0.0036	0.0033	0.0052
duty of heater [kW]	3.59	3.43	3.75	3.57
duty of reboiler [kW]	335	293	305	269
duty of cooler [kW]	211	208	181	182
duty of pump 1 [kW]	0.52	0.55	0.52	0.55
duty of pump 2 [kW]	9.2	9.7	9.2	9.7

References

[1] dos Santos L.C., Abunahman S.S., Tavares F.W., Ruiz Ahón V.R., Kontogeorgis G.M., *Cubic Plus Association Equation of State for Flow Assurance Projects,* Industrial & Engineering Chemistry Research, 2015, 54, 6812-6824.

[2] Petropoulou E.G.,Voutsas E.C., Thermodynamic Modeling and Simulation of Natural Gas Dehydration Using Triethylene Glycol with the UMR-PRU Model. *Industrial & engineering chemistry research* 2018. DOI: 10.1021/acs.iecr.8b01627

4. Economic evaluation

Following the optimization of the process in terms of energy requirements, a preliminary economic evaluation of the unit has taken place. To this purpose, the Aspen ICARUS Economic evaluator has been used with the parameters as presented in Table 4.1. In order to evaluate the results of the Aspen HYSYS, the required installation costs calculated through generalized correlations taken from the literature have been also conducted. [1-3]

Before starting the HYSYS economic evaluation, some changes have been made to the simulation environment:

1) The start date for the simulation has been set to January 2017
2) The operating hours has been set to 8000 h/year
3) The equipment material has been set to stainless steel 304

The use of stainless steel is justified according to Campbell [4] especially in the parts that get into contact with the rich TEG stream. The latter is a precaution, in order to avoid corrosion of the equipment, especially in case of sour gases. It should be noted that for the calculation of the capital cost with HYSYS, the same correlation used in the detailed analysis is considered in order to avoid the use of assumptions for labor hours, shifts etc. that are not necessary in this preliminary analysis. However, the values calculated in this way, are compared with the detailed value calculated through HYSYS.

Fixed capital cost (C) is based on an estimate of the purchase cost of the major piece of equipment required by the process (C_e), and of other costs as: equipment erection, piping, electrical power and lighting, instruments and automatic process control systems, process buildings and structures, offices, laboratory buildings, storage for raw materials, site preparation. These additional costs have been estimated as factors of each equipment cost (F).[2]

The fixed capital cost of a plant (C) has been estimated as a function of the total purchased equipment cost by eq. 4.1 [1]:

$$C = \sum_{i=1}^{i=M}(F * C_e) \qquad \text{(Eq. 4.1)}$$

Where:

- C is total capital cost of the plant
- C_e is the purchased cost of each major equipment item
- *F* is an installation factor specified for each major piece of equipment.

The equipment cost C_e has been estimated by eq. 4.2 [1]:

$$C_e = a + b * S^n \qquad \text{(Eq. 4.2)}$$

Where:

- C_e is the purchased equipment cost
- *a* and b are cost constants taken from Towler and Sinnott [2]
- S is the size parameter
- n is an exponent for that type of equipment, taken from Towler and Sinnott [2].

The specific size parameter for each piece of equipment, and the values of *a*, b and n constants, which correspond to cost at year 2006, are taken by Towler and Sinnott and are reported in Table 4.1 [2] .

Table 4.1 Size parameter and values of *a*, b, n and F constants corresponding to year 2006 [2]

		Units for Size, S	*a*	b	n	F
Vessels	Vertical, carbon steel	shell mass, kg	400	230	0.6	4
	condenser	area, m^2	500	1100	1	
Trays	Sieve	diameter, m	100	120	2	2.5
Heat exchangers	U-tube, shell & tube	area, m^2	10000	88	1	3.5
	thermosiphon reboiler	area, m^2	13000	95	1	
Pumps	Single-stage centrifugal	flow Liters/s	3300	48	1.2	4
	Explosion-proof motor	power, kW	920	600	0.7	

The purchased equipment cost has been then corrected with a material factor (f_m=1.3 for stainless steel), as per eq. 4.3, since stainless steel has been used instead of carbon steel to avoid corrosion, especially in the presence of hydrogen sulfide. For what concerns the pressure, the only equipment in which there was a deviation from the base conditions was the contactor. However, since the size parameter used to estimate the purchased cost was the shell mass, it took into account the higher wall thickness required due to the higher pressure. For this reason, also in the work of Neagu et al. [1], there is not a corrective factor for the pressure.

$$C_{e,SS} = C_e \cdot f_m \qquad \text{Eq. (4.3)}$$

Then, the equipment cost estimated has been updated to the year 2017 with the Chemical Engineering Plant Cost Index (CEPCI) with the relationship of Eq. 4.4: [1] The cost obtained using the correlations of the literature is referenced as "ours" in the following results, while the one calculated through Aspen ICARUS software as "HYSYS".

$$C_{e,2017} = C_{e,2006} * \frac{CEPCI_{2017}}{CEPCI_{2006}} \qquad \text{Eq. (4.4)}$$

Where:

- $CEPCI_{2006} = 478.6$ [1]
- $CEPCI_{2017} = 567.5$ [1]

The main units of the equipment which have been considered for the calculation of the capital cost of plant are: the contactor, the regenerator, the flash drum, the glycol cooler, the glycol/glycol heat exchangers and the glycol pumps.

The sizing of the equipment is taken from Aspen HYSYS. In the case of heat exchangers, though, a direct calculation of the size parameter, which is the heat transfer

area, occurs as per eq 4.5, by considering a design heat transfer coefficient equal to 0.3 kW/m^2 ^{o}C [2]

$$Q = U * A * \Delta T_{lm} \qquad \text{Eq. (4.5)}$$

Where:

- Q is the heat transferred per unit time (kW)
- U is the overall heat transfer coefficient (kW/m^2 ^{o}C)
- A is the heat transfer area (m^2)
- ΔT_{lm} is the mean logarithmic temperature difference (^{o}C)

The duty is the one calculated through the HYSYS simulations, while the ΔT_{lm} has been calculated in detail. With the multiplication of a corrective factor (ε) this value was the same of that given by HYSYS. The heat transfer area calculated with equation 4.5 is close to that estimated through the economic evaluation of HYSYS.

4.1 Estimation of the total equipment and capital costs

In order to make a comparison between our calculations and the results of Aspen economic evaluation, the capital cost of HYSYS has been obtained by multiplying the equipment cost given by HYSYS for the same F factor mentioned above. The results are also compared with those calculated directly through Aspen ICARUS software.

Tables 4.2 and 4.3 show the equipment and installed costs given by Aspen HYSYS and those calculated with the formulas mentioned above for the simulation with TST-NRTL model for base and optimized operating conditions respectively.

Table 4.2 Equipment and capital costs for base operating conditions with TST-NRTL model with two different ways of calculation, ours and HYSYS

equipment type	S	C_e ($) (ours)	C_e ($) (HYSYS)	C ($) (ours)	C ($) (HYSYS) ($C_e$*F)	C ($) (HYSYS) calculated by software
heat exchanger 1	9.07	16645	10900	58258	38150	65200
heat exchanger 2	11.26	16943	11000	59299	38500	66400
cooler	8.28	16538	10900	57882	38150	62300
Reboiler	11.22	21682	15100	75887	52850	72200
contactor	5579	63366	40500	253462	162000	188200
sieve trays	1.5	1711	-	4278	-	-
total contactor	-	65077	-	257740	-	-
flash drum	1361	27528	17800	110112	71200	107400
regenerator	1089	24156	18900	96623	75600	142400
sieve trays	1.5	1711	-	4278	-	-
total regenerator	-	25867	-	100900	-	-
pump 1	1.23	5182	3900	20728	15600	32700
pump 1, motor	0.52	2000	-	4999	-	-
total pump 1	-	7182	-	25728	-	-
pump 2	1.23	5182	-	20728	-	-
pump 2, motor	9.15	5773	-	14433	-	-
total pump 2	-	10955	52700	35161	210800	87900
total	-	208416	181700	780967	702850	824700

Table 4.3 Equipment and capital costs for optimized operating conditions with TST-NRTL model with two different ways of calculation, ours and HYSYS

equipment type	S	C_e ($) (ours)	C_e ($) (HYSYS)	C ($) (ours)	C ($) (HYSYS) ($C_e$*F)	C ($) (HYSYS) calculated by software
heat exchanger 1	18.67	17947	12500	62814	43750	53900
heat exchanger 2	8.03	16504	10400	57766	36400	52800
cooler	8.66	16589	10800	58063	37800	55800
Reboiler	11.47	21719	11500	76015	40250	49800
contactor	5534	63059	39400	252236	157600	174800
sieve trays	1.5	1711	-	4278	-	-
total contactor	-	64770	-	256513	-	-
flash drum	1361	27528	17100	110112	68400	99500
regenerator	1089	24156	17800	96623	71200	141100
sieve trays	1.5	1711	-	4278	-	-
total regenerator		25867	-	100900	-	-
pump 1	1.24	5183	3900	20730	15600	32700
pump 1, motor	0.52	2000	-	4999	-	-
total pump 1	-	7182	-	25729	-	-
pump 2	1.24	5183	51800	20730	207200	84700
pump 2, motor	9.16	5779	-	14447	-	-
total pump 2	-	10961	-	35177	-	-
total	-	209068	175200	783090	678200	745100

It is observed that according to the calculations based on the generalized formulas, a higher by 0.3% equipment cost is required for TST-NRTL model for the optimized conditions, which corresponds to about 650$. This is attributed to the higher heat exchange area required at the first glycol/glycol heat exchanger. Actually, the required area is double compared to the base conditions. Although in a first glance the cost seems higher, this leads to sufficient savings at operating cost due to the better use of the available heat of the hot streams, as it is shown in Section 4.2, while its amount is actually insignificant compared to the total equipment cost. The calculations by HYSYS instead, result to a 3.6% decrease

of the equipment cost. This reduced cost is based on significant reduction of the regenerator and flash drum costs. Instead, in the case of our calculations, the size parameters used for the estimation of the equipment costs have been actually constant and the difference was based mostly on the heat exchanger calculations.

For both considered cases, the equipment costs calculated based on our calculations and the HYSYS ones are about 50%. Exception is the duty of the pump-2, where HYSYS calculates an order of magnitude value higher compared to our calculations. Yet, as a total, the equipment cost as calculated through correlations is about 15% higher compared to that of HYSYS for base conditions and 19% higher for optimized conditions, using the TST-NRTL model.

In terms of capital cost, a difference of about 23% is observed when the capital cost of HYSYS is calculated with the appliance of the *F* factor to the equipment cost. This is actually rational, since the difference of the equipment cost is directly reflected on the capital one. Instead, if the values directly calculated by Aspen ICARUS software for the capital cost, a 5% difference is observed. The latter is valid for both base and optimized conditions with the TST-NRTL model.

In the case of UMR-PRU model, the equipment cost for the optimized conditions is very similar to that obtained for the base ones. The calculated costs differ by 0.03%, which corresponds to a reduction by 50$, which is trivial if the overall cost of the process and the uncertainty of the calculations are considered. Since UMR-PRU yields systematically lower duties compared to TST-NRTL, due to the lower calculated heat capacity for TEG-rich streams, the required area for the heat exchangers in both conditions is lower. Although, again, in optimized conditions higher exchange area is required, this is about 1.6% of a lower value, which corresponds to lower increase of the equipment costs. As it was the case for TST-NRTL, the size parameters calculated by HYSYS for most of the

units, with the exception of heat exchangers, are again the same and thus the equipment cost is similar to that of the base conditions (Tables 4.4 – 4.5).

Table 4.4 Equipment and capital costs for optimized operating conditions with UMR-PRU model: comparison with HYSYS

equipment type	S	C_e ($) (ours)	C_e ($) (HYSYS)	C ($) (ours)	C ($) (HYSYS) ($C_e$*F)	C ($) (HYSYS) calculated by software
heat exchanger 1	8.25	16534	10300	57868	36050	51600
heat exchanger 2	7.96	16494	10200	57729	35700	52800
cooler	7.93	16490	10200	57716	35700	53900
Reboiler	10.30	21547	11300	75414	39550	50800
contactor	5534	63059	47400	252236	189600	184300
sieve trays	1.5	1711	-	4278	-	-
total contactor	-	64770	-	256514	-	-
flash drum	1361	27528	16800	110112	67200	100900
regenerator	1089	24156	18100	96623	72400	142400
sieve trays	1.5	1711	-	4278	-	-
total regenerator	-	25867	-	100900	-	-
pump 1	1.26	5184	4500	20736	18000	33400
pump 1, motor	0.55	2025	-	5063	-	-
total pump 1	-	7209	-	25800	-	-
pump 2	1.26	5184	53200	20736	212800	86300
pump 2, motor	9.73	5966	-	14915	-	-
total pump 2	-	11150	-	35651	-	-
total	-	207589	182000	777704	707000	756400

If the results between our calculations and those of HYSYS are considered, we result at the same observations as it was for TST-NRTL. That is, an about 50% higher equipment cost for all units, apart from the pump-1, where a reduced cost of 70% is

calculated through HYSYS. Again, in the total equipment cost a 18% higher is calculated by the correlation compared to that of HYSYS. This is actually reflected on the capital cost as it is calculated through the *F* factors. Instead, if the capital cost obtained by HYSYS is considered, an about 3% deviation is observed between our and HYSYS calculations. The same observations are valid for the optimized conditions as well. So, it is concluded that the total equipment and capital costs calculated through our calculations and HYSYS are overall in good agreement.

Table 4.5 summarizes the total equipment and capital costs calculated with both considerations, as well as the corresponding deviations.

Table 4.5 Comparison between the total equipment and capital costs

	Ce ($)		C ($)			% deviation* of C_e from HYSYS	% deviation (C)	% deviation from HYSYS (C)
	ours	HYSYS	ours	HYSYS (Ce*F)	HYSYS calculated by software		HYSYS (Ce*F)	HYSYS calculated by software
TST-NRTL base	208416	181700	780967	702850	824700	15	23	-5
TST-NRTL optimized	209068	175200	783090	678200	745100	19	15	5
UMR-PRU base	207638	177200	778041	687400	749700	17	13	4
UMR-PRU optimized	207589	182000	777704	707000	756400	14	10	3

* deviation is calculated as: $\%deviation = \frac{C_{ours} - C_{HYSYS}}{C_{HYSYS}} \cdot 100$, where stands for equipment or capital cost

As it has been mentioned in section 2.4, the simulation is based on a synthetic wet gas with composition and flow taken from the literature. Since for the calculation of the cost the capacity of the unit should be taken into consideration, the previous results are reduced to costs per standard cubic meters of treated gas (scm) in order to be compared with literature values. [3] Table 4.6 presents the reduced equipment and installed cost per standard cubic meter of treated wet gas. The wet gas rate in MMscmd (millions of standard cubic meter per day) is reported in the first column, since it is different between the two

models due to the different density that they calculate and is approximately equal to 38.2 MMscfd for both models.

Table 4.6 Comparison between the total equipment and capital costs for standard cubic meter of dry gas

	Dry gas molar flow (MMscmd)	Ce ($/scm) (ours)	Ce ($/scm) (HYSYS)	C ($/scm) (ours)	C ($/scm) (HYSYS)
TST-NRTL base	38.194	0.00546	0.00476	0.02045	0.01840
TST-NRTL optimized	38.195	0.00547	0.00459	0.02050	0.01776
UMR-PRU base	38.188	0.00544	0.00464	0.02037	0.01800
UMR-PRU optimized	38.188	0.00544	0.00477	0.02036	0.01851

The costs estimated from the economic evaluation have been compared with some values extracted from two graphs [3,5]. These two graphs report the total capital cost of the dehydration unit on the vertical axes, and the plant capacity on the horizontal axis. The first graph analyzed is reported in Figure 4.1 [3]. The value extrapolated for 1999 has been updated to 2017 through the index CEPCI. For a plant capacity of 38.2 MMscmd the total capital cost is about 400000$ for year 1999 and is updated to 580000$ for the year 2017.

Following the similar procedure, from Figure 4.2 [5] it is extracted a capital cost of 600000$ for year 2008 which, updated to 2017, corresponds to 680000$.

The deviation from the costs calculated and those given by HYSYS, in the case of optimized operating conditions with UMR-PRU model, is 34 % compared to ours calculations, and of 22% compared with the results of HYSYS (the total equipment cost of HYSYS has been calculated as C=Ce*F as mentioned at the beginning of this section).

The capital cost extrapolated from this graph is closer to the results of HYSYS. In estimating the capital cost through the graph in Figure 4.1, some assumption has been done. The cost does not include some costs which could range from 25% to 40% of the plant cost (miscellaneous equipment associated with grassroots plant site and site preparation cost, home office cost, interest on investment during construction, construction insurance or bond cost) [3]. The percentage of the costs which are not included is closer to the percentage

of deviation from our calculations and the results of the HYSYS economic evaluation in the case of optimized operating conditions with UMR-PRU model. If the UMR-PRU optimized conditions is considered, a 35% deviation from the value of the graph based on 1999 is observed through our calculations. Instead, the deviation from HYSYS using the *F* factors approach is 22% while from HYSYS by software 30%. According to Carrol [6] a 30% uncertainty is expected from the values presented on this graph, so our calculations are in general good agreement and rational. The deviation from the results of 2008, is lower in all considered cases, since the estimated value from the graph is higher compared to 1999. Actually, it is 15% based on "our" calculations, 4% based on HYSYS with the F factors approach and 11% as calculated directly from HYSYS software.

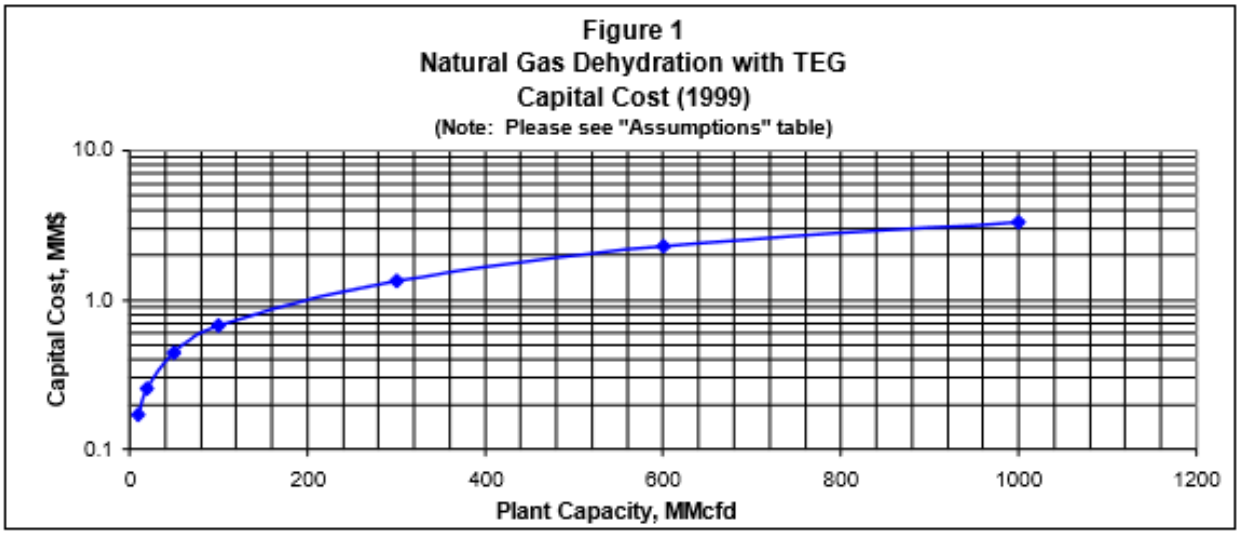

Figure 4 .1 Capital cost of natural gas TEG dehydration unit for year 1999 [3]

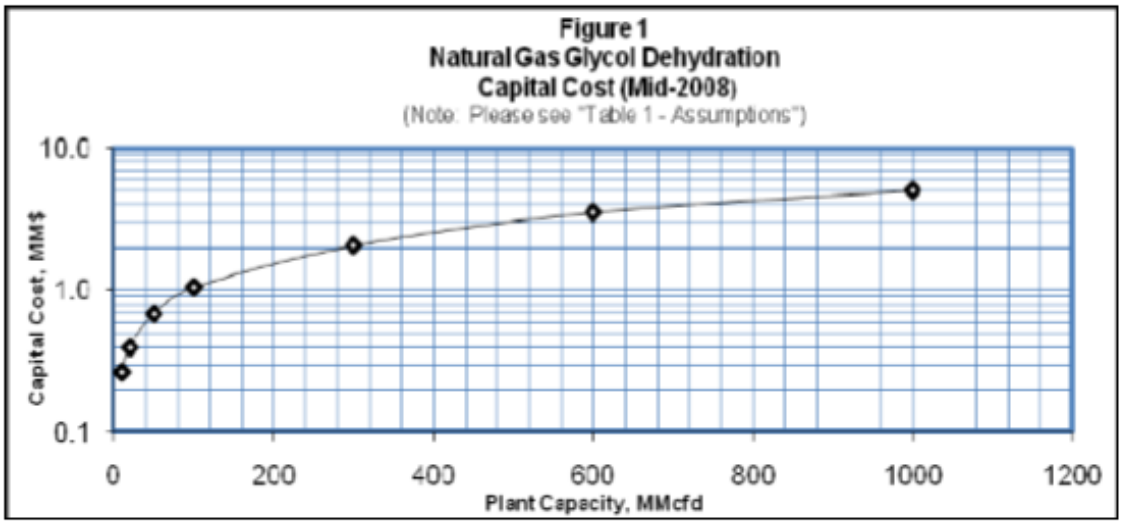

Figure 4 .2 Capital cost of natural gas TEG dehydration unit for year 2008 [5]

4.2 Estimation of the utilities cost

In this section an estimation of the utilities cost needed by the process has been done, in order to compare both the difference between the operating conditions and the performances of the two thermodynamic models. The utilities considered in this work are:

- High pressure saturated steam, for the reboiler, due to its high temperature requirement.
- Cooling water, for the cooler.
- Electricity, for the pumps.

For the above mentioned utilities, some costs have been found from different sources. The values are reported in Table 4.7 where, in the first row, the reference number has been reported.

Table 4.7 Utilities cost taken from different literature sources

Utilities	[5]	[7]	[2]	[8]	[1]	HYSYS
High Pressure steam [$/ton]	4.4	7.95	-	30	-	5.09
Cooling Water [$/ton]	0.08	0.26	0.005	-	0.135	0.0044
Electricity [$/kWh]	0.045	0.07	0.06	-	0.1	0.077

In order to do a preliminary estimation, the most reasonable values have been chosen. In particular, for the high pressure steam the cost is of 30 $/ton [8], which includes the cost for its production, the cooling water costs 0.08 $/ton [5] and the price for electricity is 0.07 $/kWh [7].

Eq. 4.6 has been used to estimate the utilities cost. [1]

$$utility\_cost\ \left[\frac{\$}{year}\right] = rate * utility\_cost\ \left[\frac{\$}{ton}\right] \qquad \text{(Eq. 4.6)}$$

Tables 4.8 and 4.9 show respectively the utilities rate and cost, expressed in dollars per year, for the base and optimized simulations with TST-NRTL and UMR-PRU models.

Table 4 8: Utilities rate for base and optimized conditions with TST-NRTL and UMR-PRU models.

Utility	Rate (TST-NRTL base)	Rate (TST-NRTL optimized)	Rate (UMR-PRU base)	Rate (UMR-PRU optimized)
High Pressure steam	701 kg/h	637 kg/h	619 kg/h	568 kg/h
Cooling Water	35710 kg/h	30189 kg/h	35850 kg/h	31472 kg/h
Electricity	106 kW	106 kW	106 kW	106 kW

Table 4.9: Utilities cost for base and optimized conditions with TST-NRTL and UMR-PRU models.

Utility	Utility Cost	Cost ($/year) (TST-NRTL base)	Cost ($/year) (TST-NRTL optimized)	Cost ($/year) (UMR-PRU base)	Cost ($/year) (UMR-PRU optimized)
High Pressure steam	30 $/ton	168318	153093	148659	136502
Cooling Water	0.08 $/ton	22855	19322	22944	20142
Electricity	0.07 $/kWh	59503	59503	59503	59503
Total cost	-	250676	231918	231107	216148

From the results shown in the tables below, we can conclude that the optimized simulation required lower utilities rates compared to the base, as it was expected. In particular, TST-NRTL model requires 10% lower high pressure steam and 18% lower cooling water, instead the percentages for UMR-PRU model are 9% and 14% respectively. This percentage of difference between base and optimized conditions has been calculated as:

$$\%difference = \frac{rate_{base} - rate_{optimized}}{rate_{optimized}} * 100$$

The abovementioned results lead to a decrease of the utilities cost for both the models. In particular, a great difference occurs between the optimized conditions of the two models, since UMR-PRU needs a smaller amount of high pressure steam for the reboiler due to its lower duty. Actually, for TST-NRTL a decrease of 8% is obtained between base and optimised conditions, while for UMR-PRU this corresponds to 7%. Although this difference seems relative small, if the total cost values are considered they correspond to a saving of about 19000$ annually for TST-NRTL model and 15000 $ annually for UMR-PRU. This difference seems rather small for an industrial procedure, but since the considered capacity is relatively small, this corresponds to about 7% of the annual operating cost. Furthermore, if the results of the optimized processes are compared, UMR-PRU model leads to 15000 $ annually saving compared to TST-NRTL.

Figure 4.3 shows the comparison between the total utilities cost, estimated with our calculations, of the simulation with base and the optimized operating conditions of the two thermodynamic models.

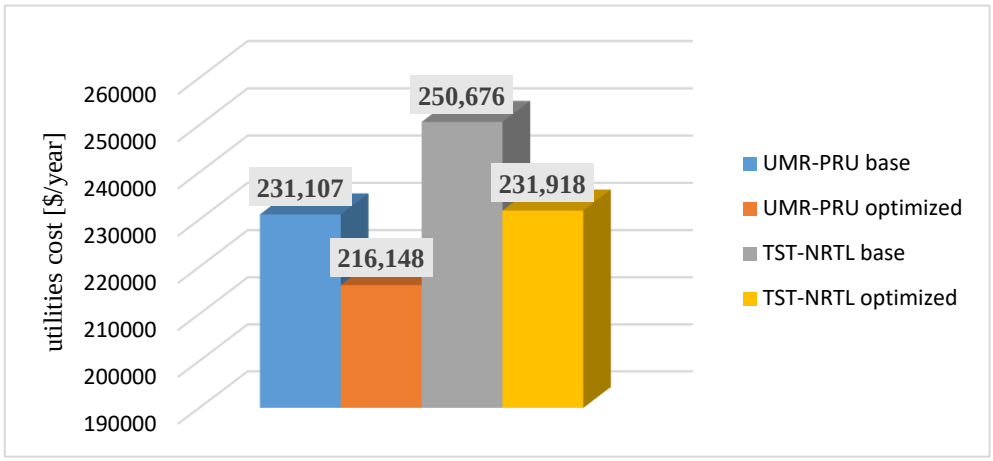

Figure 4.3 Comparison between the utilities cost of base and optimized conditions of the two models (our calculations)

Since the main difference between the four cases is on the high pressure steam required, in Figure 4.4 are reported the costs of this specific utility in $/year.

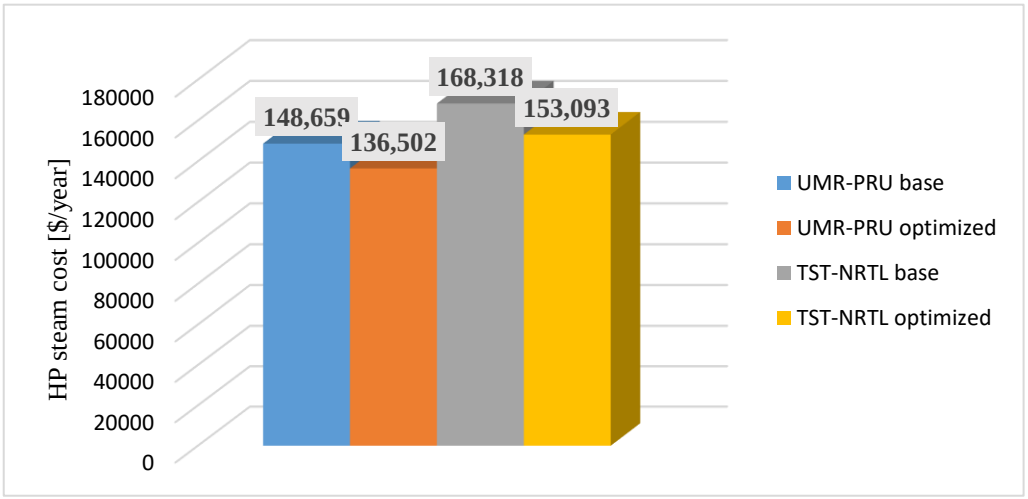

Figure 4. 4 Comparison between the HP steam cost of base and optimized conditions of the two models (our calculations)

Following the results of the calculation made, we can sum up the following conclusions:

- 8% lower utilities cost for the optimized operating conditions with TST-NRTL model, compared to the base conditions.

- 7% lower utilities cost for the optimized operating conditions with UMR-PRU model, compared to the base conditions.

- 7% lower utilities cost for the simulation with UMR-PRU compared to TST-NRTL, both for optimized operating conditions. This difference is due to the lower amount of HP steam required by the simulation with UMR model, since the reboiler duty required is lower.

- 12% lower amount of HP steam required by UMR-PRU, compared to TST-NRTL, both for optimized conditions.

4.3 References

[1] Neagu M., Cursaru D.L., Technical and economic evaluations of the triethylene glycol regeneration processes in natural gas dehydration plants, Journal of Natural Gas Science and Engineering, 2017, 37, 327-340

[2] Towler, G., Sinnott, R., Chemical Engineering Design: Principle, Practice and Economics of Plant and Process Design. Butterworth-Heinemann Elsevier Ltd, United Kingdom, 2008.

[3] Tannehill, C.C., Budget Estimate Capital Cost Curves for Gas Conditioning and Processing, Proceedings of the Seventy-Ninth Annual Convention of the Gas Processors Association RR-141, Tulsa, OK, 2000

[4] Campbell, J.M. and Maddox R.N., Gas conditioning and processing. Vol. 2. Campbell Petroleum Series. 1970.

[5] Max S. Peters, Klaus D. Timmerhaus, Ronald E. West, “Plant design and economics for chemical engineers”, 5th ed., ΕΚΔΟΣΕΙΣ ΤΖΙΟΛΑ, 2001

[6] Carroll, J., Natural Gas Hydrates: A Guide for Engineers. Gulf Professional Publishing, Elsevier: USA, 2003.

[7] Max S. Peters, Klaus D. Timmerhaus, "Plant design and economics for chemical engineers", 4th ed., McGraw-Hill International Editions, 1991

[8] Turton R., Analysis, synthesis and design of chemical processes, fourth edition, section 2: engineering economic analysis of chemical processes, Prentice Hall, 2012.

5. Real gas

In this chapter the performance of the two models has been compared in a simulation with a real gas stream as input. The difference is in the composition of the wet gas stream is on the presence of pseudo-components to account for the undefined compounds of high molecular weight, which are less than 1% of the total gas, as well as in the capacity of the considered unit. The composition of the wet gas stream is reported in Table A.13 in Appendix.

The flowsheet of the dehydration unit, as simulated on HYSYS, is reported in Figure 5.1. There is a difference in the pre-treatment for the wet gas stream than the previous flowsheet. In particular, an inlet cooler and valve have been added in order to reach the contactor operating conditions. The inlet cooler reduces the wet gas temperature from 85^{o}C so the temperature of the inlet scrubber is set to 27^{o}C. Additionally, a JT-valve reduces the pressure from 87 bar to 52 bar. The inlet scrubber has been considered to avoid the presence of a liquid phase entering the contactor along with the gas stream. Thus it is ensured that only saturated wet gas enters as input to the contactor.

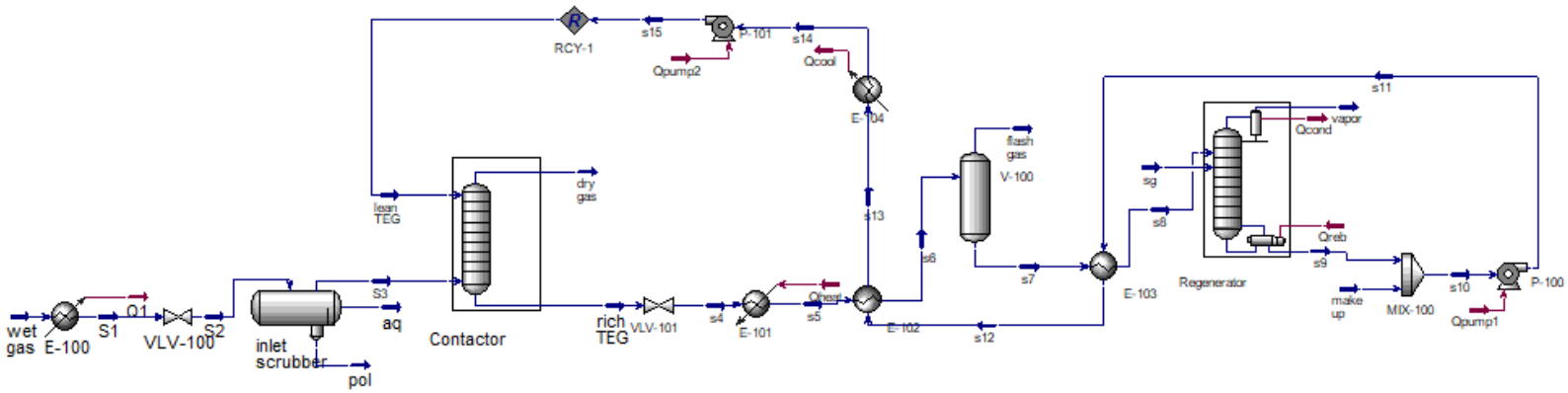

Figure 5.1 Flowsheet of natural gas TEG dehydration unit for a real stream.

The operating conditions set for the simulations with the two models are reported in Table 6.2. In order to compare this simulation with the other results of the work, the specification to be met is the same (30 ppm as dry gas water content). There is a great difference between the simulations with the two models, due to a higher amount of lean TEG rate required by TST-NRTL model to meet the specification of 30 ppm as dry gas water content. The other operating parameters set were the same for both the simulations, as it is shown in Table 5.1.

Table 5.1 Operating conditions set for simulations with a real gas for TST-NRTL and UMR-PRU models.

OPERATING CONDITIONS	TST-NRTL	UMR-PRU
reboiler temperature [°C]	204.6	204.6
reboiler pressure [bar]	1.27	1.27
flash drum temperature [°C]	75	75
regenerator temperature [°C]	130	130
contactor temperature [°C]	27	27
contactor pressure [bar]	51.65	51.65

The results obtained with the simulations with the two models are reported in Table 5.2.

Table 5.2 Simulations results with for a real gas stream with TST-NRTL and UMR-PRU models.

	TST-NRTL	UMR-PRU
stripping gas molar flow [kmol/h]	482	394
lean TEG purity [mol]	0.962	0.955
lean TEG molar flow [kmol/h]	2100	2100
dry gas water content [ppm]	30.7	30.9
dry gas TEG content [ppm]	0.35	0.65
TEG loss [kmol/h]	0.236	0.273
duty of heater [kW]	283	169
duty of reboiler [kW]	20616	17343
duty of cooler [kW]	16384	14909
duty of pump 1 [kW]	32	33
duty of pump 2 [kW]	560	577

As it is reported in Table 5.2, the results of this comparison between the two models are in good agreement with those obtained with the previous analysis with the synthetic gas. The main difference between the two thermodynamic models is on the calculated duties, where, as it was in the previous case UMR-PRU model yields lower values compared to TST-NRTL. This is more apparent in the case of the reboiler and cooler duties, since the difference on the values required by the two models is very marked.

Actually it is about 19% in the reboiler case and 10% for the cooler. As observed in the synthetic gas case, the models differ also in the calculated stripping gas rate, which in this case is more profound due to the higher rates considered. In particular, TST-NRTL model requires a higher amount of stripping gas rate to reach the specification of 30 ppm as dry gas water content, which is 22% higher than that required by UMR-PRU model. Yet, both models result in similar lean TEG purity. However, a slight difference is observed for the calculated TEG loss, which is higher in the case of the UMR-PRU model. As it has been stated in Section 3, the TEG loss calculated with the UMR-PRU model is expected to be closer to the actual process data due to better prediction of the TEG solubility in methane. [1] Furthermore, it is resulted that the molar flow of the three streams which exit the three flash separator is almost the same for the two models.

The distribution of pseudo-components in the three gas streams vented off the unit is presented in Figures 5.2 – 5.4. The analysis was done at a basis of 100 kmol/h as mole flow in order to have a good comparison between the compositions of the streams.

In Figure 5.2 the dry gas pseudo-component content is shown for both the models.

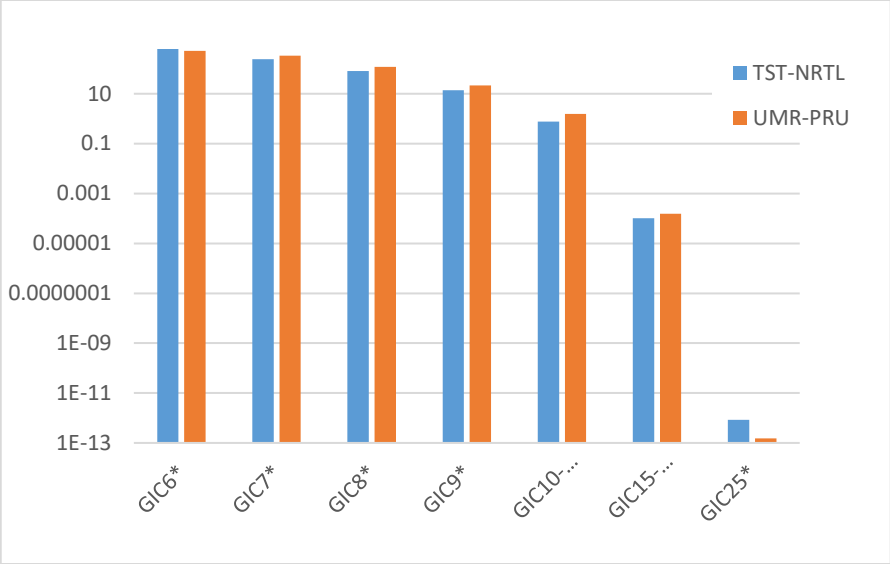

Figure 5. 2 Distribution of pseudo-components in dry gas

In Figure 5.3 the flash gas pseudo-components content is reported. In this case, these components have higher solubility in the gas phase with UMR-PRU model, resulting thus in higher hydrocarbon loss, except for the heaviest component. The phase equilibria of aqueous-hydrocarbon and TEG-hydrocarbon mixtures are better predicted with UMR-PRU, in both polar and hydrocarbon-rich phase. Actually, UMR-PRU yields higher hydrocarbon solubility in aqueous phase compared to TST-NRTL, especially for the heavier hydrocarbons. [1] It is thus, concluded that the hydrocarbon loss calculated with UMR-PRU should be closer to the actual process data.

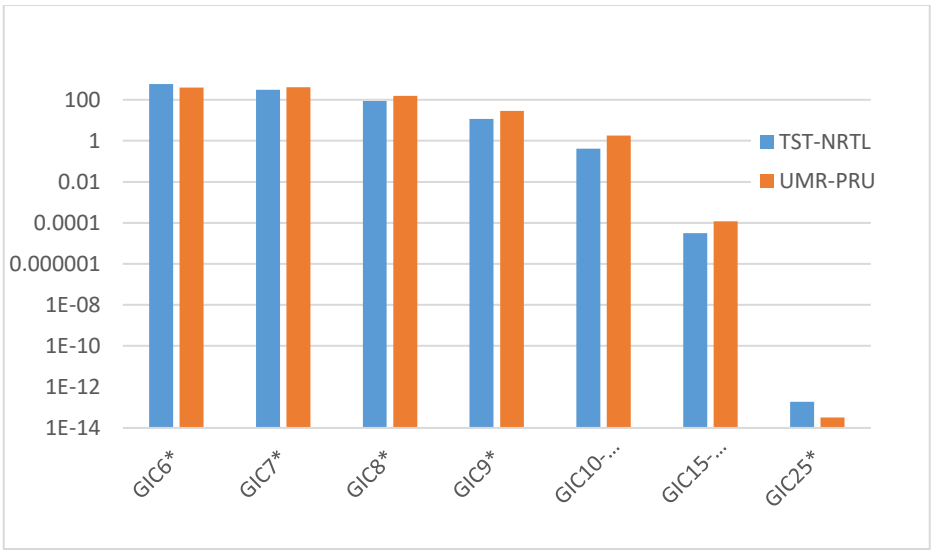

Figure 5 3 Distribution of pseudo-components in flash gas

In Figure 5.4 the vapor stream pseudo-components content is reported. Also in this case, higher solubility in the gas phase is observed with UMR-PRU model, especially for the heaviest component.

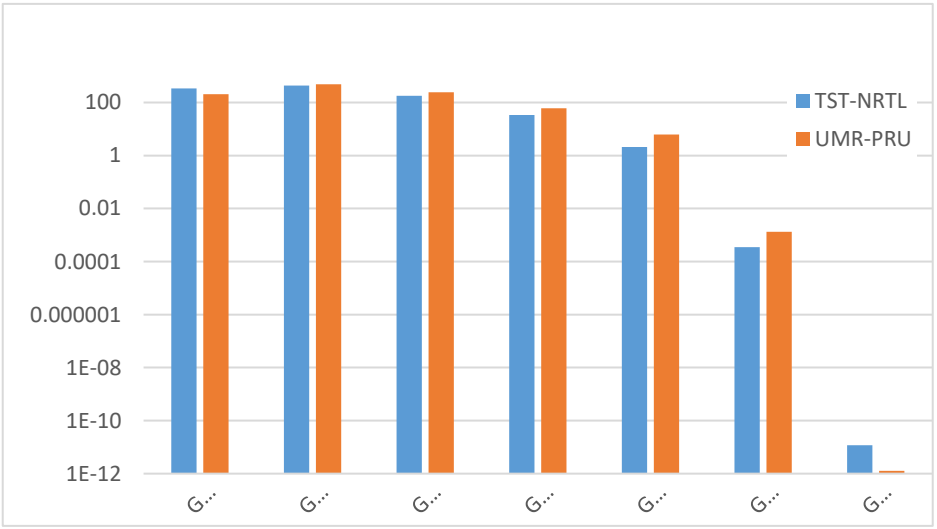

Figure 5. 4 Distribution of pseudo-components in vapor stream exiting the regenerator

To conclude, the results obtained by the simulation with a real gas stream are in agreement with those obtained previously with the simulation of a synthetic natural gas. In particular, the simulation with UMR-PRU model requires lower duties

compared to those of the simulation with TST-NRTL model, as effect of the different performances of the two thermodynamic models in the prediction of the heat capacities. Overall, both models yield similar results in terms of lean TEG purity, but in contradiction to the previous simulation this is obtained by slightly different requirements in terms of TEG circulation rate and stripping gas rate. Furthermore, from the analysis of the distribution of pseudo-components in the gaseous streams, it can be concluded that generally these components have higher solubility in the gas phase with the UMR-PRU model.

References

[1] Petropoulou E.G.,Voutsas E.C., Thermodynamic Modeling and Simulation of Natural Gas Dehydration Using Triethylene Glycol with the UMR-PRU Model. *Industrial & engineering chemistry research* **2018**. DOI: 10.1021/acs.iecr.8b01627

6. Conclusions

In this work Aspen HYSYS simulation software has been used, in order to do a sensitivity analysis and to compare the performances of two thermodynamics models in the simulation of a natural gas dehydration plant using TEG absorption. Namely, the TST-NRTL which is a built-in HYSYS model and the UMR-PRU added into HYSYS through the CAPE-OPEN 1.1 protocol have been considered.

The following operating variables have been considered for the sensitivity analysis: the operating temperature and pressure of contactor and regenerator, the stripping gas rate, the flash drum temperature, the temperature of the rich TEG stream entering the regenerator. It is concluded that both models yield similar results regarding the effect of the parameters in the total process.

Following the results of the sensitivity analysis, an optimization of the process in terms of the required duties has been conducted by increasing the flash drum temperature and the temperature of the rich TEG stream which enters at the bottom of the regenerator. The optimized conditions have been compared to the base ones, in terms of calculated duties, for a process with the specification of about 30 ppm molar of water in the dry gas stream. To this purpose, the stripping gas rate has been used as the independent variable. The simulation results showed reduced duties with both models, namely 9% for TST-NRTL and 8.2% for UMR-PRU.

Furthermore, a preliminary economic evaluation of the unit has been considered, by calculating the capital and the operational cost. To this purpose the Aspen ICARUS software implemented in the HYSYS environment is considered and the obtained results are compared with results based on correlations from the literature. Actually the latter are based on relationships based on previously installed units, using the sizing of the equipment. It is concluded that the capital cost calculated by HYSYS and through the correlations is very similar, deviating at about 5% in all examined cases. The costs calculated by both models do not substantially differ between the base and optimized conditions. The obtained results have been also compared with literature values for

dehydration units and they are shown to be in good agreement, with an about 15% obtained with UMR-PRU at optimized conditions. In terms of the operating cost, an 8% decrease has been obtained in the optimized simulation for the TST-NRTL model and a 7% for the UMR-PRU. This corresponds to a saving of about 15700$ in annual basis, which is about 7% of the total operational cost.

Finally, the performance of the models has been evaluated in the simulation of the TEG dehydration plant using as input a real rather than a synthetic natural gas. The difference from the previous case, is apart from the heavier and actually undefined components included in the gas, also to the considered plant capacity. Both models result in similar performance in terms of lean TEG purity in the case where they result in a water content of 30ppm in the dry gas. Nevertheless, they differ in the calculated stripping gas rate. Overall, the results are considered successful in both examined cases and similar to those obtained for the synthetic gas stream. The difference of the models is more apparent in this case, where higher molecular components are considered, in the distribution of the heavier hydrocarbons in glycol-rich streams. UMR-PRU yields systematically higher hydrocarbon loss compared to TST-NRTL, which is considered closer to the actual process data due to better prediction of the corresponding phase equilibrium of aqueous-hydrocarbon mixtures. UMR-PRU yields higher TEG loss compared to TST-NRTL and in the this case. Instead, the duties calculated with UMR-PRU are lower, as a result of the lower calculated heat capacity, as it was expected based on the simulation of the synthetic gas.

To conclude, the UMR-PRU model can accurately simulate the dehydration of natural gas by absorption with TEG. The models yield similar results in terms of TEG circulation rate, TEG purity and the parametric analysis of the variables which affect the process efficiency. Instead, they differ in the calculated duties, hydrocarbon and TEG loss. Due to better prediction of the respective properties with the UMR-PRU model, it is considered that its simulation results should better meet the actual process data.

Overall, the UMR-PRU model yields better results in the simulation of a natural gas dehydration unit than the proposed by HYSYS, TST-NRTL model and it is considered a robust and accurate model to be used for such simulation.

7. Future work

Although, many studies have been conducted for the natural gas TEG dehydration process, several questions remain unanswered. Future work on the field can consider the following:

- To obtain field data, so that the simulations can be compared to the actual results. This could be of special interest for the parameters where the model performance differs, such as the calculated duties.
- Other variables of the sensitivity analysis can be also considered, such as the number of trays in contactor or regenerator.
- To evaluate the contemporary influence of two or more parameters on the whole process.
- To make an economic evaluation of the simulation with a real gas, in order to have a better comparison with the reality.
- To make a comparison of both performances and costs, between the process with stripping gas and other processes such as vacuum distillation, since the obtained results are primarily dependent on the lean TEG purity.
- To evaluate the addition of another heat exchanger to obtain more efficient exchanger of heat between the lean and rich TEG streams.

Appendix

Table A. 1 Results of the analysis after variations of the reboiler temperature (TST-NRTL model)

reboiler temperature [°C]	lean TEG purity [wt]	lean TEG molar flow [kmol/h]	dry gas water content [ppm]	heater duty [kW]	reboiler duty [kW]	cooler duty [kW]	pump 1 duty [kW]	pump 2 duty [kW]
200	0.994	35.7	30.13	3.58	317	191	0.52	9.2
202	0.994	35.6	30.1	3.58	325	201	0.52	9.2
204	0.994	35.5	29.99	3.59	335	210	0.52	9.2
204.5	0.994	35.3	29.98	3.59	338	212	0.52	9.2
205	0.994	35.3	29.96	3.59	340	214	0.52	9.2
206	0.994	35.3	29.94	3.59	344	219	0.52	9.2

Table A 2 Results of the analysis after variations of the reboiler temperature (UMR-PRU model)

reboiler temperature [°C]	lean TEG purity [wt]	lean TEG molar flow [kmol/h]	dry gas water content [ppm]	heater duty [kW]	reboiler duty [kW]	cooler duty [kW]	pump 1 duty [kW]	pump 2 duty [kW]
200	0.994	35.3	28.36	3.58	275	190	0.54	9.7
202	0.994	35.3	28.33	3.58	283	198	0.54	9.7
204	0.994	35.3	28.3	3.58	291	206	0.54	9.7
204.5	0.994	35.3	28.29	3.58	294	209	0.54	9.7
205	0.994	35.3	28.28	3.58	295	210	0.54	9.7
206	0.994	35.3	28.26	3.58	299	214	0.54	9.7

Table A .3 Results of the analysis after variations of the reboiler pressure (TST-NRTL model)

Condenser temperature [°C]	reboiler pressure [bar]	lean TEG purity [wt]	lean TEG molar flow [kmol/h]	dry gas water content [ppm]	TEG loss [kmol/h] E-04	heater duty [kW]	reboiler duty [kW]	cooler duty [kW]	pump 1 duty [kW]	pump 2 duty [kW]
70	0.1	0.99	33.6	0.7	8.51	10.13	368	208	0.76	9.1
70	0.2	0.99	33.9	4.7	5.26	3.85	356	202	0.74	9.1
70	0.3	0.98	34.2	7.5	4.51	3.08	352	203	0.72	9.1
80	0.4	0.97	34.4	10.0	4.48	2.39	349	203	0.70	9.2
80	0.5	0.96	34.7	12.4	4.36	2.10	346	203	0.68	9.2
85	0.6	0.95	35.0	14.8	4.36	1.74	343	204	0.66	9.2
90	0.7	0.95	35.3	17.2	4.43	1.41	340	205	0.64	9.2
95	0.8	0.94	35.6	19.5	4.47	1.11	337	205	0.62	9.2
95	0.9	0.93	35.9	21.8	4.25	0.89	334	206	0.60	9.2

Table A. 4 Results of the analysis after variations of the reboiler pressure (UMR-PRU model)

Condenser temperature [°C]	reboiler pressure [bar]	lean TEG purity [wt]	lean TEG molar flow [kmol/h]	dry gas water content [ppm]	TEG loss [kmol/h] E-04	heater duty [kW]	reboiler duty [kW]	cooler duty [kW]	pump 1 duty [kW]	pump 2 duty [kW]
70	0.1	0.999	33.3	0.52	38.8	3.03	308	207	0.79	9.64
70	0.2	0.998	33.6	5.79	13.8	2.55	298	200	0.77	9.63
70	0.3	0.997	34.9	11.07	9.89	2.04	295	201	0.75	9.63
80	0.4	0.996	34.2	16.29	9.78	1.61	292	201	0.73	9.63
80	0.5	0.995	34.5	21.69	9.42	1.26	289	202	0.70	9.62
85	0.6	0.994	34.9	27.04	9.62	0.89	286	203	0.68	9.62
90	0.7	0.993	35.2	32.39	9.85	0.56	283	205	0.66	9.62
95	0.8	0.992	35.5	37.77	1.02	0.26	280	206	0.64	9.62
95	0.9	0.991	35.8	43.17	1.00	0.11	279	206	0.62	9.62

Table A. 5 Results of the analysis after variations of the flash drum temperature (TST-NRTL model)

temperature of the flash drum [°C]	lean TEG purity [wt]	dry gas water content [ppm]	heater duty [kW]	reboiler duty [kW]	cooler duty [kW]	pump 1 duty [kW]	pump 2 duty [kW]
50	0.993	30.5	3.6	334	209	0.52	9.2
55	0.993	30.5	3.6	334	209	0.52	9.2
65	0.993	30.02	3.6	334	209	0.52	9.2
75	0.993	29.97	3.6	334	208	0.52	9.2
80	0.993	29.94	3.6	334	208	0.52	9.2
85	0.993	29.89	3.6	333	208	0.52	9.2
90	0.993	29.82	3.6	333	208	0.52	9.2
95	0.993	29.75	3.6	333	208	0.52	9.2
100	0.993	29.65	3.6	333	207	0.51	9.2
110	0.993	29.43	3.6	332	207	0.51	9.2

Table A. 6 Results of the analysis after variations of the flash drum temperature (UMR-PRU model)

temperature of the flash drum [°C]	lean TEG purity [wt]	dry gas water content [ppm]	heater duty [kW]	reboiler duty [kW]	cooler duty [kW]	pump 1 duty [kW]	pump 2 duty [kW]
50	0.994	28.40	3.60	294	209	0.55	9.7
55	0.994	28.39	3.60	294	209	0.55	9.7
65	0.994	28.36	3.59	294	209	0.55	9.7
75	0.994	28.29	3.59	294	209	0.55	9.7
80	0.994	28.23	3.58	294	208	0.55	9.7
85	0.994	28.17	3.58	294	208	0.55	9.7
90	0.994	28.09	3.58	294	208	0.55	9.7
95	0.994	28.00	3.58	293	208	0.55	9.7

Table A 7 Results of the analysis after variations of the input regenerator temperature (TST-NRTL model)

input regenerator temperature [°C]	lean TEG purity [wt]	lean TEG molar flow [kmol/h]	dry gas water content [ppm]	heater duty [kW]	reboiler duty [kW]	cooler duty [kW]	pump 1 duty [kW]	pump 2 duty [kW]
110	0.990	36.3	50	1.0	419	294	0.52	9.2
115	0.991	35.9	44	1.6	398	273	0.52	9.2
120	0.992	35.6	32	2.2	377	252	0.52	9.2
125	0.993	35.3	34	2.9	356	231	0.51	9.2
130	0.994	35.0	29	3.5	335	210	0.51	9.1
135	0.995	34.8	26	4.3	314	190	0.51	9.1
140	0.995	34.6	22	5.0	294	169	0.51	9.1

Table A. 8 Results of the analysis after variations of the input regenerator temperature (UMR-PRU model)

input regenerator temperature [°C]	lean TEG purity [wt]	lean TEG molar flow [kmol/h]	dry gas water content [ppm]	heater duty [kW]	reboiler duty [kW]	cooler duty [kW]	pump 1 duty [kW]	pump 2 duty [kW]
110	0.990	36.5	48	0.9	362	277	0.55	9.7
115	0.991	36.2	42	1.5	345	260	0.55	9.7
120	0.992	35.8	37	2.2	328	243	0.55	9.7
125	0.993	35.6	32	2.8	311	226	0.55	9.7
130	0.994	35.3	28	3.5	294	209	0.55	9.7
135	0.995	35.1	24	4.3	277	192	0.55	9.7
140	0.995	35.0	21	5.1	259	174	0.55	9.7

Table A 9 Results of the analysis after variations of the contactor temperature (TST-NRTL model)

Contactor temperature [°C]	lean TEG purity [wt]	dry gas water content [ppm]	dry gas TEG content [ppm]	reboiler duty [kW]	cooler duty [kW]	pump 1 duty [kW]	pump 2 duty [kW]
13	0.9936	15.32	0.06	420	234	0.52	9.25
16	0.9937	17.91	0.08	419	248	0.52	9.24
20	0.9937	21.85	0.11	419	265	0.52	9.24
25	0.9938	27.69	0.17	419	287	0.52	9.24
27	0.9939	30.32	0.20	418	295	0.52	9.23
30	0.9939	34.71	0.26	418	308	0.52	9.23
35	0.9941	43.01	0.37	417	329	0.52	9.21
40	0.9942	52.72	0.54	416	350	0.52	9.20
45	0.9944	63.93	0.77	415	370	0.51	9.18
50	0.9946	76.69	1.10	413	390	0.51	9.15

Table A 10 Results of the analysis after variations of the contactor temperature (UMR-PRU model)

contactor temperature [°C]	lean TEG purity [wt]	dry gas water content [ppm]	dry gas TEG content [ppm]	reboiler duty [kW]	Cooler duty [kW]	pump 1 duty [kW]	pump 2 duty [kW]
13	0.9938	13.35	1.49	294	172	0.54	9.73
16	0.9938	15.92	1.82	294	180	0.54	9.73
20	0.9939	19.91	2.37	294	191	0.54	9.73
25	0.9940	25.97	3.25	294	204	0.54	9.73
27	0.9940	28.77	3.68	294	210	0.54	9.73
30	0.9941	33.38	4.43	294	218	0.54	9.73
35	0.9942	42.26	5.98	293	232	0.54	9.73
40	0.9944	52.74	8.02	293	246	0.54	9.73
45	0.9946	64.88	10.66	293	260	0.54	9.73
50	0.9948	76.68	14.07	292	274	0.54	9.73

Table A .11 Results of the analysis after variations of the contactor pressure (TST/NRTL model)

contactor pressure [bar]	lean TEG purity [wt]	dry gas water content [ppm]	dry gas TEG content [ppm]	reboiler duty [kW]	cooler duty [kW]	pump 1 duty [kW]	pump 2 duty [kW]
50	0.993	29.62	0.18	332	205	0.51	9.1
52	0.993	29.71	0.20	332	209	0.51	9.1
55	0.993	30.35	0.25	332	216	0.51	9.1
57	0.993	30.84	0.28	332	220	0.51	9.1
60	0.993	31.45	0.34	332	226	0.51	9.1
62	0.993	31.86	0.38	332	230	0.51	9.1
65	0.993	32.50	0.46	331	236	0.51	9.0
67	0.993	32.94	0.52	331	240	0.51	9.0
70	0.993	33.62	0.62	331	245	0.51	9.0

Table A .12 Results of the analysis after variations of the contactor pressure (UMR-PRU model)

contactor pressure [bar]	lean TEG purity [wt]	dry gas water content [ppm]	dry gas TEG content [ppm]	reboiler duty [kW]	cooler duty [kW]	pump 1 duty [kW]	pump 2 duty [kW]
50	0.994	27.9	3.33	294	206	0.55	9.7
52	0.994	28.37	3.67	294	209	0.55	9.7
55	0.994	29.12	4.22	294	213	0.55	9.7
57	0.994	29.64	4.63	294	216	0.55	9.7
60	0.994	30.44	5.3	294	220	0.55	9.7
62	0.994	31.00	5.79	294	223	0.55	9.7
65	0.994	31.85	6.58	294	227	0.55	9.7
67	0.994	32.43	7.16	294	230	0.55	9.7
70	0.994	33.32	8.09	294	234	0.55	9.7

Table A 13 Real gas composition (wet gas based)

Component list	kmol/h
Nitrogen	115
CO_2	1260
Methane	26200
Ethane	3340
Propane	1610
i-Butane	288.3
n-Butane	469.1
i-Pentane	127.3
n-Pentane	122
GIC6*	115
GIC7*	127
GIC8*	84.6
GIC9*	30.6
GIC10-C14*	14.6
GIC15-C24*	0.269
GIC25*	5.77E-05
H_2O	257.7
Total molar flow	34196